

**Visual feedback from the own acting hand modulates the activity of grasping
neurons in monkey premotor area F5**

Luana Caselli¹, Andriy Oliynyk¹, Benno Gesierich¹, Laila Craighero¹ and Luciano Fadiga^{1,2}

¹ Department of Biomedical Sciences and Advanced Therapies, University of Ferrara, Ferrara, Italy

² The Italian Institute of Technology, Genova, Italy

Running head: Visual feedback and grasping neurons

Address for correspondence:

Professor Luciano Fadiga

Department of Biomedical Sciences and Advanced Therapies

Section of Human Physiology, University of Ferrara

Via Fossato di Mortara 17/19

44100 Ferrara, Italy

luciano.fadiga@unife.it

ABSTRACT

Visual responses in the monkey ventral premotor cortex have been explored since long time. Area F5 has been shown to contain grasping neurons that visually discharge either to 3D-object presentation (canonical neurons) or to the observation of actions performed by other individuals (mirror neurons). It has been suggested that the mirror response results from the progressive generalization to others' actions of a visuomotor link which, during action execution, associates the vision of the own acting effector with the motor program selected for the ongoing action. To start tackling this hypothesis, we specifically asked whether area F5 contains neurons responding to the observation of one's own grasping movement. A specially-designed experimental apparatus was used to test F5 neuronal discharge while monkeys were engaged in a reach-to-grasp task and either continuous or transient visual information on the ongoing movement was made available. Single-unit activity was additionally recorded from the hand region of the primary motor cortex (area F1). Neuronal responses evoked by the vision of the own entire grasping action or of brief meaningful phases of it were detected in both areas. However, F5 modulation was overall more strong and specific. The finding that neurons in area F5 exhibit discharge properties that are common to both purely motor and mirror neurons allows the formulation of important assumptions about the critical role of online visual information during grasping and the nature of the mirror discharge.

INTRODUCTION

Visual responses in the premotor cortex have been extensively studied in the last two decades. Thereby, ventral premotor area F5, residing in the posterior bank and convexity of the inferior arcuate sulcus (iAS), has turned out to be particularly important for the visuomotor transformations it carries out in the domain of visually-guided grasping movements (Murata et al. 1997; Raos et al. 2006; Rizzolatti et al. 1988). Grasping is one of the most evolved types of primate behavior, resulting from a complex visuomotor process that transforms the object's three-dimensional structure into specific motor commands to select the optimal finger configuration for grasping. During pre-shaping, fingers progressively open and straighten up to reach a point of maximum grip aperture, which is followed by closure of the grip with gradual finger flexion as the hand approaches the object (Jeannerod et al. 1995).

Intracortical microstimulation and single-unit recordings in the macaque monkey have demonstrated that cortical control of grasping relies on a fronto-parietal visuomotor circuit including, besides area F5, the inferior intraparietal area AIP (Murata et al. 1996, 2000), the ventro-rostral part of area F2 in the dorsal premotor cortex (Raos et al. 2004) and the primary motor cortex F1 (Dum and Strick 2005; Umiltà et al. 2007). Successful execution of grasping much depends on the integrity of area F1, which directly controls finger muscles and is known to be crucial for skilled hand function. Lesions or inactivation of this area produce a severe deficit of individual finger movements and, consequently, of normal grasping (Fogassi et al. 2001, Liu and Rouiller 1999). F5, which provides through cortico-cortical connections one of the major inputs to the hand field of area F1 (Matelli et al. 1986), is the motor region most critically involved in pre-shaping the hand according to the visual properties of the object. After inactivation of area F5, hand shaping is markedly impaired, with fingers position not properly matching the size and shape of the object (Fogassi et al. 2001).

In addition to purely motor grasping neurons, which are typically goal-oriented and specify types of grasping (e.g., precision or whole-hand grip) or time the action discharging during different grasping phases, two main categories of F5 visuomotor neurons have been described so far. On the basis of their visual properties they have been named *canonical* and *mirror* visuomotor neurons.

Canonical neurons, mainly located in the posterior bank of the iAS (F5ab sector), display a 3D object-related visual selectivity that is almost congruent with the grip-specificity of their motor discharge. *Mirror* neurons, mainly sited on the F5 cortical convexity (F5c), are visually triggered by the observation of a biological agent performing a given goal-directed action (e.g. grasping). They therefore *mirror* the motor response normally recorded from the same neurons during the actual action execution (di Pellegrino et al. 1992; Gallese et al. 1996, Rizzolatti et al. 1996). The matching between the observed and the executed action encoded by a single mirror neuron response has been shown to encompass different levels of congruence, ranging from a very strict to a broader visuomotor correspondence. Broadly congruent mirror neurons are of particular interest since they generalize the goal of the observed action over many instances of it. For example, neurons whose motor discharge is selective for a precision grip can either only respond to the observation of actions involving the same precision grip or be visually triggered by any type of hand grasping. Another example concerns the relative point of view-independency characterizing the response of some mirror neurons. It has been shown that the vision of the same grasping action performed with different orientations of the hand elicits comparable discharges from a given recorded neuron (Gallese et al. 1996). This peculiar property of F5 mirror neurons suggests that different visual information (i.e., different perspectives of the observed acting hand) are associated to a common goal-related motor-invariant signal for grasping at the single-neuron level.

These observations and the fact that mirror neurons are part of a cortical circuit, additionally including the PF/PFG complex in the inferior parietal lobule (Fogassi et al. 2005; Fogassi and Luppino 2005; Matelli et al. 1986; Petrides and Pandya 1984) and the superior temporal sulcus

(STS) (Perrett et al. 1989), which describes actions in purely visual terms, have led to the formulation of a sensory feedback-based theory accounting for the generation of mirror neurons (Rizzolatti and Fadiga 1998). According to this theory, the mirror discharge may develop from the observation of one's own acting effector, seen from slightly different perspectives, performing repetitively the same action. Given that for the agent, the goal of a specific action is independent from his/her own point of view while performing the action, it is likely that, motor invariance is progressively extracted from the different action perspectives through the visual feedback system normally guiding action execution. so to create an automatic matching between execution and observation of one's own ongoing actions. Once this visuomotor link has been established, this generalization process could work also during the observation of actions executed by other individuals. Very recent results, achieved by testing this model with an acting artificial system, show that this could be the case (Craighero et al. 2007; Metta et al. 2006).

Hence, according to the feedback-based theory, a prerequisite to the generation of the mirror neurons' response would be the existence, in area F5, of neurons showing visuomotor responses associating the execution with the observation of one's own actions.

So far, neurons with such properties have not been described in area F5. Own hand observation-related responses have been previously reported in area AIP in the inferior parietal lobule, which is directly connected to F5ab (Luppino et al. 1999). These AIP neurons (*nonobject-type* neurons) devoid of any object-related visual selectivity, were shown to significantly increase their activity when the monkey observed its own grasping action (i.e., under full light conditions), with respect to grasping in darkness (Murata et al. 2000; Sakata et al. 1995). These discharge properties have been thought to be related to the vision of the grasping hand or to a combined view of the object and of the correspondingly selected handgrip. This interpretation supports the claim that visual feedback is of unquestionable importance in goal-directed hand movements, especially for the formation of finger grip during prehension (Jeannerod 1986; Jeannerod et al. 1995).

The aim of the present study was to investigate the existence in area F5 of “*nonobject-type-like*” neurons, whose motor discharge is specifically modulated by the vision of the acting hand, in the absence of any canonical- or mirror-like visuomotor properties.

To minimize the risk that significant differences in activity between grasping in light and grasping in dark were due to kinematic differences in executing the grasping under the two conditions (Rand et al. 2007; Winges et al. 2003), we kept the to-be-grasped object back-illuminated and, more importantly, we introduced two conditions of phasic visual stimulation (i.e., light flashes delivered at precise instants during grasping in dark) that do not alter arm/hand kinematics with respect to the dark condition, though providing the motor system with strategically useful visual information. As a final control, the activity of neurons in the hand representation of primary motor cortex F1 was recorded as well.

METHODS

Surgery

Single-unit activity was recorded from both ventral premotor area F5 and primary motor cortex F1 in three hemispheres (contralateral to the moving forelimb) of two awake behaving monkeys (*Macaca fascicularis*). The monkeys (one female and one male, respectively weighing 5.7 kg and 4.9 kg and referred as to MK1 and MK2) were specifically trained to perform a behavioral task (see following text), while seating on a primate chair. After training, a recording chamber and head-restraint device were surgically implanted. All experimental protocols were approved by the Ethical Committee of the University of Ferrara, by the Italian Ministry of Health and complied with the European laws on the use of laboratory animals.

Structural CT and MRI images were respectively used in MK1 and MK2 to stereotactically place the recording chamber over the cortical region including the posterior bank of the inferior arcuate sulcus and central sulcus, where areas F5 and F1 are located. In MK1, the cortical surface was indirectly rendered after Computer Assisted Tomography (CAT) acquisition, through reversal of inner skull surface, and 3D-reconstructed by using ETDIPS (NIH, NUS, <http://www.cc.nih.gov/cip/software/etdips/>) and Rhinoceros[®] 2.0 (Robert McNeel & Associates, USA) softwares. The coordinate system of the obtained 3D-images of the brain was then adjusted to the standard stereotaxic coordinates system based on the orbitomeatal plane and with a custom-designed software (Virtax, <http://web.unife.it/progetti/neurolab/>, Gesierich et al., in preparation) we determined the position of the target cortices by using as references both the sulcal pattern impressed on the internal surface of the skull and the stereotaxic atlas by Szabo and Cowan (Szabo and Cowan 1984). The inferior surface of the titanium recording chamber cylinders (height 20 mm, inner \varnothing 24 mm, out \varnothing 30 mm) was virtually modeled through Rhinoceros[®] 2.0 software, so to perfectly fit the skull curvature of the monkeys, maximizing adhesion between the implant and the

bone. The chamber models were then manufactured by a MAXNC 15 computer-driven 3D milling machine (MAXNC inc., Arizona, U.S.A.), using the MillWizard software (Delcam Artcam, U.K.).

All surgical implantations were carried out under aseptic procedures and general anesthesia. Monkeys were pre-medicated with atropine sulfate (0.1 mg/Kg, IM, MONICO S.p.A., Italy) and tiletamine-zolazepam (20 mg/Kg, IM, Zoletil, VIRBAC, S.A., France), and then anesthetized by isoflurane (Abbott S.p.A., Illinois, U.S.A.) for the whole duration of surgery. Antibiotics and analgesics were administered postoperatively and experiments were started at least two weeks after the surgery.

Electrophysiology

Single-unit recordings were performed by using varnish-insulated tungsten microelectrodes with impedance 0.15–1.5M Ω (measured at 1 kHz). Electrodes were obtained repetitively passing the tip of tungsten rods (\varnothing 250 μ m, A-M Systems, inc. WA, U.S.A.) through an etching solution (10% KOH in distilled water) by means of a metal electrode etcher (BAK Electronics, inc., MD, U.S.A.), and covering them with multiple layers (between 8 and 12) of polyamideimide-based enamel (SIVAMID 595/38M, ELANTAS Electrical Insulation, Germany) that were oven-dried at high temperature (400°C, 15 s per layer). This procedure has the advantage of providing microelectrode tips with a highly resistant insulation.

During each experimental session, the microelectrode was inserted perpendicular to the cortical surface (i.e., with an angle of 32-40° with respect to sagittal plane) and was slowly advanced through the cortex by means of a hydraulic microdrive (Kopf Instruments, CA, U.S.A.; step resolution, 10 μ m). The recorded signal was amplified \times 10000 (BAK Electronics, Germantown MD, USA), filtered by a dual variable filter (VBF-8, KEMO Ltd., Backenham, UK) (300-5000 Hz bandwidth), digitized at a sampling rate of 10 kHz (PCI-6071E, National Instruments, USA) and stored on hard disk for further off-line analysis. During recordings, action

potentials were on-line discriminated by a dual-voltage time-window discriminator (BAK Electronics, Germantown MD, USA) and fed to an Audio monitor (Grass Instruments, USA) to give the experimenter an auditory feedback on the neuron discharge during testing. Single-units were off-line discriminated from multi-spike recordings by means of a custom-made LabView-based software (Olyinik et al., in preparation). Data analyses were performed by using MATLAB 7.2., R2006a (The Mathworks Inc.).

The recording microelectrodes were also used for intracortical microstimulation (ICMS, train duration, 50-100 ms; pulse duration, 0.2 ms; frequency, 330 Hz; current intensity, 3–40 μ A). The current strength was controlled on an oscilloscope by measuring the voltage drop across a 10 k Ω resistor in series with the stimulating electrode.

Recording sites

The rostro-caudal and medio-lateral dimensions of the recording chamber were such as to allow to record from a brain region including area F1, the whole ventral premotor cortex and the caudal part of the Frontal Eye Fields (FEF). The ventral part of the agranular frontal cortex was functionally explored through single unit recordings and ICMS to assess the location of areas F1, F4 and F5. Criteria and functional characteristics described by Umiltà et al. (2001) were used to distinguish motor and premotor areas as well as regions within area F5 characterized by a high density of neurons exhibiting hand-related activity during goal-directed actions.

Naturalistic testing

Naturalistic testing was used to select neurons to be then thoroughly examined through the experimental paradigm. Single-neuron activity was studied with reference to the execution of different hand/arm movements, selected to elicit different grip types or to the application of different sensory stimuli, according to the procedures described in previous studies (Gallese et al.

1996; Rizzolatti et al. 1988; Rizzolatti et al. 1990). For example, the presentation of a small piece of food placed inside a groove required the monkey to perform a precision grip, by opposing the first phalanx of the thumb to the first phalanx of the index finger, while a syringe filled with juice evoked a power grip, with the fingers wrapped around the object and the palm in contact with it. Visual canonical properties were tested by presenting the monkey with 3D objects of different size, shape and orientation. Visual mirror properties were tested by performing a series of hand actions (e.g., grasping holding, manipulating) in front of the monkey. This functional characterization, together with the ICMS data, allowed us to select hand-related neurons predominantly selective for precision grasping. Particular attention was paid so to discard cells showing any kind of canonical or mirror visual properties and to include in the present study just those neurons showing only motor responses.

Behavioral apparatus and paradigm

The pre-selected grasping neurons were studied by means of a behavioral apparatus specifically designed to make the animals perform a reach-to-grasp task, which naturally implied the execution of a precision grip to open the door of a container and get a piece of food which was hidden inside (Fig. 1A). The container was mounted on a vertical rack at reaching distance (approximately 30 cm) in front of the primate chair, so that, in case, the monkeys were allowed to see their own grasping trajectory. The precision grip had to be performed on a small plastic cube (0.8 x 0.8 x 0.8 mm) embedded in a groove, serving as the door handle (Fig. 1B). To ensure that the movement was accurately executed even under dark conditions, the cube was translucent and dimly back-illuminated by a red LED. The LED intensity was kept very low and did not allow the vision of the approaching hand. Each trial started with the monkey's right (or left) hand positioned close to the body, on the hip board of the primate chair. An external sliding door, overlying the target door for the animal, was opened at distance by the experimenter, giving the monkey a go-signal to start

the reach-to-grasp movement (Fig. 1C). As the monkey touched the handle correctly, with both the thumb and index finger, a TTL signal was sent via an electronic circuit to the acquisition PC to synchronize the neuronal data. Data included one second before and two seconds after handle grasping were stored for each trial.

The task was performed under four different conditions:

- 1) *Light (L)* condition: grasping was executed with continuous vision of the own hand movement (i.e., in full light).
- 2) *Dark (D)* condition: grasping was executed in absence of any visual information on the own movement (i.e., in darkness).
- 3) *Pre-touch (PT) flash* condition: grasping was executed in dark with instantaneous visual feedback before handle touching, during the hand pre-shaping phase. The scene was briefly illuminated by a 20 μ s xenon light flash triggered by the signal of the hand crossing an infrared barrier built by a pyroelectric sensor located 10 cm in front of the food container.
- 4) *Touch (T) flash* condition: grasping was executed in dark with instantaneous visual feedback at hand-handle contact. The scene was briefly illuminated by a 20 μ s xenon light flash delivered as both the thumb and index finger touched the target handle.

Experimental conditions were presented in blocks of twelve trials and administered with the same temporal order (described above) in all sessions. Figure 1D shows a schematic representation of the time sequence of task events under the 4 different conditions.

The *Light* condition was repeated at the end of each recording session just to confirm the stability of neuronal activity (*Light 2* condition).

Hand kinematics acquisition

During specific sessions, the behavioral task was administered to MK1 and kinematics of the arm/hand was recorded in the different grasping conditions. Markers were placed on the wrist to

evaluate the transport component of the movement and on the last phalanx of the thumb and index finger to measure grip aperture during hand shaping (Jeannerod et al. 1995). After a first brief period of familiarization with the markers, the monkey was able to execute the experimental task naturally. Twelve kinematic recordings were collected for each experimental condition. The three-dimensional trajectories of each marker were acquired (240 frames/sec) by an infrared-sensitive motion tracking system (ProReflex/Qualisys Track Manager, Qualisys AB, Sweden).

Spike sorting

The isolation of single neurons from multispikes recordings was performed off-line by using Singular Value Decomposition of the data matrix containing the different spike waveforms, followed by Fuzzy C-mean clustering analysis of Principal Components in the multi-dimensional space (Oliylyk et al., in preparation). The good quality of the discrimination was confirmed by evaluating the single-unit interspike interval histograms and the main quantitative parameters of cluster quality, including L_{ratio} measures (Bezdek et al. 1984; Lewicki 1998; Schmitzer-Torbert et al. 2005). A custom-made software was created for this purpose and all implemented algorithms were entirely realized by LabVIEW 7.0 software (National Instruments, U.S.A.). An additional library for LabVIEW (DataEngine V.i library, MIT GmbH, Germany) was used to implement the Fuzzy C-mean clustering.

Analyses

Kinematics

The 3D position over time of wrist, thumb and index fingertips was off-line reconstructed by Qualisys Track Manager software (Qualisys AB, Sweden) and the following kinematic parameters were determined for each condition: wrist velocity, grip aperture, deceleration time, defined as the

time interval between the peak of wrist velocity and the instant of target touch, and finger closure time, defined as the time interval between the occurrence of the maximal grip aperture and target touch instant. A non-parametric one-way ANalysis Of VAriance –ANOVA- (*Kruskal-Wallis test*, 5% alpha level) was performed to compare *Light*, *Dark*, *PT flash*, *T flash* and *Light 2* conditions for each of these parameters.

Single neurons

The first analysis performed on the dataset aimed at determining the presence of task-related modulation of neuron discharge. To this purpose, the difference in activity between baseline (*epoch 1*) and the movement-related epoch (*epoch 2*) was statistically assessed in all conditions for each neuron by means of a two-way repeated-measure ANOVA (5% alpha level) with *epoch* (*epoch 1* and *epoch 2*) and *condition* (*D*, *L*, *PT flash* and *T flash*) as factors. *Epoch 1* corresponded to a pre-movement period, during which the hand was about to initiate the movement from the starting position (first 500 ms in the trial); *epoch 2* corresponded to a 500-ms grasping-related period including both the hand shaping and finger closure phases, going from 250 ms before the instant at which the hand touched the target handle (*pre-touch* sub-epoch) to 250 ms after it (*post-touch* sub-epoch). Neurons which did not show any significant difference in firing rate between *epoch 1* and *epoch 2* in any condition (i.e., conjunct lack of *epoch* main effect and of significant differences between epochs within one particular condition, as resulting from the *Tukey's Least Significant Difference* (LSD) post-hoc tests performed on significant *epoch x condition* interactions) were discarded from further analyses.

To assess whether neurons' activity was modulated by the vision of the own acting hand, data analyses were first focused on detecting differences in activity between *D* and *L* conditions in *epoch 2*. In order to better appreciate even subtle effects in activity, a two-tail paired *Student's t-test* (5% alpha level), comparing *D* vs. *L* mean firing rates, was performed on individual neurons on a

running 100-ms bin, stepped through the trial by 20-ms increments. Figure 4D shows the output of this analysis performed on the *D* and *L*-related activity of two single cells taken from the F5 and F1 recorded neuronal samples (Fig. 4C). A neuron was considered as significantly modulated if it displayed a statistically significant difference in activity between the two conditions in at least three consecutive time bins. According to the direction of the effect shown in the *pre*- and *post-touch* sub-epochs of *epoch 2*, each neuron was then classified as positively or negatively modulated by light in both or either of the two sub-epochs.

To investigate the effect of the light flashes on grasping-related neuronal activity, a similar approach was employed. In view of the fact that *PT flash* and *T flash* were transient visual manipulations and represented hybrid situations with respect to the *D* and *L* conditions as for both physical and functional aspects, direct comparisons between activity during either flash condition and *D* (or *L*) were avoided at the first-level analysis. This choice was also driven by the purpose of getting rid of any unspecific arousal-related flash effect. Thus, the above described running *t-test* analysis was used to contrast single-neuron discharge in *PT flash* and *T flash* conditions, with the aim to primarily identify neurons firing preferentially when a light flash was delivered at a specific relevant instant in the trial. In particular, we were interested in any firing difference observed between the two flash conditions within *epoch 2*, with the idea that, even a very short-lived visual information, if relevant for the ongoing hand movement, should modulate the grasping-related activity of the neuron. Once flash-selective neurons were detected, their flash-related activity was compared with the activity they exhibited in the *D* and *L* condition and thoroughly studied at the population level.

Estimation of neuronal response latency and peak. Response latency was calculated using a version of the time to half-height of the peak nonparametric technique (Gawne et al. 1996), which detects the midpoint between the minimum and maximum values of the single-neuron firing rate histogram, smoothed with the optimal bandwidth. We chose to implement this technique because it

gives a latency measure which is less susceptible to noise than the one obtained through other methods computing latency at the onset of the neuronal response, when the rate of change in activity is quite low and therefore characterized by an unfavorable signal-to-noise ratio. By definition, the maximum firing value in the histogram is the peak of neuronal discharge. The single-neuron spike train, averaged and aligned with respect to the handle touch instant (time 0) for each condition, was convolved with a smoothing Gaussian kernel function with window width set at 20 ms, to obtain a spike density function (SDF) that provide a continuous and fine (1-ms binned) time-dependent measure of the firing pattern. The first time this SDF exceeded the average of the minimum and peak values in the period including the grasping movement (first 1250 ms in the trial) was regarded as the estimated response latency of the neuron in one given experimental condition.

Neuronal populations

Normalization was achieved for each neuron composing a population through ms-by-ms dividing the smoothed SDF relative to one given experimental condition by the highest discharge value (peak of activity) observed across all four conditions. Population plots were obtained by averaging the normalized smoothed SDF of the included neurons.

Statistical analyses on the activity recorded within a specific trial period (e.g., *pre-touch* or *post-touch* sub-epoch) during particular conditions were carried out on the single-neuron mean raw firing rates in the target period, normalized to the maximum activity across all four conditions, as just described.

Analyses on latency or peak firing rates were performed assigning to each entry in a given pre-selected population, the normalized activity values respectively corresponding to the time of half-maximum or maximum activity (see above) for each single unit.

Estimation of neuronal latency of light- and flash-selectivity. The same method used for computing single-neuron motor response latency was employed to calculate the neuronal latency of

light and flash selectivity expressed at the population level. In this case, latency was defined as the time at which firing in *L* vs. *D* (or in *PT flash* vs. *T flash*) trials differed from one another in a relevant way. Therefore, we compared the time at which the difference in the population activity between the two conditions under investigation reached half of the maximum value, considering the normalized mean firing rate differences computed on a sliding 100-ms bin (sliding step, 20 ms). This method was used to have an additional measure for expressing the latency of neuronal selectivity, besides the one given by the running *t-test* analysis (see above), that returns the time course of the selectivity of the neuronal population.

Estimation of magnitude of light- and flash-selectivity. The strength of light- and flash-selectivity was evaluated by using a Receiver Operating Characteristic (ROC) analysis (Metz 1978; Wallis and Miller 2003), which measures the degree of overlap between two response distributions. Hence, given for instance the two distributions of neuronal activity *L* (i.e., *Light*-related) and *D* (i.e., *Dark*-related), for each observed single-neuron firing rate, the proportion of *L* against the proportion of *D* response distribution exceeding that firing rate was plotted and the area under the plotted curve (ROC area) was computed, yielding a single value for that comparison. This method has several advantages. First, it provides an assumption-free estimate of the degree of overlap between *L* and *D* distributions: values near 0.5 indicate large overlap between the distributions, whereas values close to 0 or 1 indicate small or no overlap, with every value drawn from one distribution exceeded by the other entire distribution and vice versa. Second, it can be conveniently interpreted as the performance of an ideal observer in a two-way forced choice task. Third, it is independent of the firing rate of the neuron and can thus be used to compare the activity of neurons with widely different baseline and dynamic firing rates. Population ROC area values, comparing *L* vs. *D* (or *PT flash* vs. *T flash*) distributions, were either computed every 20-ms step in a 100-ms bin covering all the trial period, or averaged within selected grasping epochs.

RESULTS

Kinematics

Arm/hand kinematics parameters acquired from MK1 were analyzed according to the procedures described in the *Methods*. Figure 2B shows the time course of wrist velocity (transport) and grip size for: Light (*L*), Dark (*D*), *Pre-touch* (*PT*) flash, *Touch* (*T*) flash and *Light 2* (*L2*).

Transport. Statistical analysis (*Kruskal-Wallis test*, 5% alpha level) on the transport component of the movement revealed that the maximal velocity was significantly higher during the *Light* conditions (*L* and *L2*) than during *PT flash* ($P < 0.02$) and *T flash* ($P < 0.05$) conditions (Fig. 2A, *Maximal velocity* plot). As a consequence, a significant shorter deceleration time was observed in full light (*L* and *L2*) with respect to all dark conditions (*Dark*, *PT flash* and *T flash*, $P < 0.0001$) (Fig. 2A, *Deceleration time* plot). Note that all these transport-related parameters were not different in the two flash conditions with respect to the dark.

Grip aperture. Maximal grip aperture was considerably larger in all dark conditions (*Dark*, *PT flash* and *T flash*) with respect to the *L* ones ($P < 0.03$) (Fig. 2A, *Maximal grip aperture* plot). This increased finger aperture under dark conditions suggests that, with reduced visual information – the target was always visible - a strategy is adopted to increase the safety margin and therefore the chances of successful grasping. This is confirmed by the fact that, after reaching the peak of maximal aperture, the fingers also closed more slowly in the dark and flash conditions than in the light ones ($P < 0.02$) (Fig. 2A, *Aperture-closure time* plot). Also in the case of the grasping-related parameters, no significant difference was observed among the dark and flash conditions. .

Overall, these findings confirm the results of previous kinematics studies on humans, reporting an increase in the duration of wrist deceleration and fingers closure phases when visual feedback was entirely or partially removed (Jackson et al. 1995; Schettino et al. 2003; Wings et al. 2003) also when the vision of the own hand only was prevented (Churchill et al. 2000; Gentilucci et

al. 1994; Rand et al. 2007; Schettino et al. 2003). The adoption of a wider maximal grip aperture in absence of any visual feedback (Jackson et al. 1995; Jakobson and Goodale 1991) or when the grasping hand was not visible (Churchill et al. 2000) has been previously described.

The fact that no kinematics dissimilarity was found between the two flash conditions (both resembling the *D* condition) demonstrates that the behavioral task employed in our work represents a valuable tool to explore the effect of the vision of the own acting hand on the response of grasping neurons in cortical motor areas.

Intracortical microstimulation

We performed 149 penetrations in three hemispheres of the two monkeys MK1 and MK2 (see Table 1). The respective functional maps are illustrated in Figure 3 (A, B, C). Figure 3D displays the three-dimensional reconstruction of the brain surface of MK2 used to position the recording chamber on the skull. Penetrations are marked according to the specific body-part movements evoked by ICMS and the current intensity threshold at which those movements were evoked. As threshold, we defined the minimal current intensity at which visually detectable movements were evoked in 50% of stimulation trials.

All sites in the rostral bank of the central sulcus (area F1) were excitable with low-threshold currents (MK1, $9.8 \pm 0.8 \mu\text{A}$; MK2, $11.4 \pm 2.2 \mu\text{A}$, mean \pm S.E.M.) evoking hand or finger movements. Microstimulation of the penetration sites rostral to F1 hand representation (estimated to be located in area F4) evoked face and axial movements at higher thresholds (MK1, $21.1 \pm 5.9 \mu\text{A}$; MK2, $27.9 \pm 3.2 \mu\text{A}$). Neurons in this region appeared to show large somatosensory receptive fields on the face and body and visual receptive fields in register with the somatosensory ones. The hand representation in area F5 was identified further rostrally, in the posterior bank of the iAS, on the basis of distal movements evoked by stimulation at the following thresholds: MK1, $24.2 \pm 2.8 \mu\text{A}$; MK2, $28.2 \pm 2.3 \mu\text{A}$. The discharge of the neurons in this region was often related to goal-directed

actions, mainly including grasping. The presence of microstimulation-induced eye movements (current intensity thresholds: MK1, 25.9 ± 4.6 ; MK2, 24.2 ± 5.7) and the recording of saccade-related activity in a region anterior to area F5 and to the iAS, were considered as functional markers of the FEF.

Inset plots within each hemisphere representation indicate the subset of penetrations where grasping motor neurons were recorded while the monkeys were engaged in performing the behavioral task. Overall, the grasping-related activity of the neuronal samples recorded from the three monkey hemispheres during the task was congruent with the functional characterization obtained through ICMS and naturalistic testing.

Neurons database

A total number of 295 and 236 grasping motor neurons were respectively isolated from F5 and F1 areas of MK1 and MK2 during 271 recording sessions. Of these neurons, 169 of area F5 (102 neurons recorded from the two hemispheres of MK1 and 67 recorded from the left hemisphere of MK2) and 128 of area F1 (106 and 22 recorded from the left hemispheres of MK1 and MK2, respectively) survived the selection criteria: stability of the recording throughout the duration of the task, sufficient number of trials recorded per each condition and activity during grasping significantly different from that displayed during the pre-movement period, as revealed by the two-way *epoch x condition* ANOVA (see *Methods*). Details concerning all recording sessions are reported in Table 1.

Dark vs. light conditions: types of neuronal modulations

We first focused on identifying neurons showing a significant difference in activity between *L* and *D* conditions during the grasping epoch. By looking at the results of the running *t-test* we found that the number of F5 neurons strengthening (22%) or diminishing (39%) their activity due to

full vision of the ongoing movement with respect to the *D* condition, mostly reflected those of F1 (22% and 32%, respectively). Neurons showing “*spurious*” effects within the same grasping epoch (see *Methods*) were 18% in area F5 and 27% in area F1. The amount of neurons which did not fire differently in the two conditions (non-modulated neurons) was comparable in the two areas (21% and 19%, respectively).

According to the period in which the neuronal modulation was observed, neurons were classified as modulated ($L>D$ or $D>L$) during the *pre-touch* sub-epoch, the *post-touch* sub-epoch, at the instant when the hand touched the handle, or through whole *epoch 2* (Tab. 2). Whereas in both areas the majority of $L>D$ effects were clustered in the *pre-touch* sub-epoch (14% in F5 and 13% in F1), the opposite modulation emerged in the *post-touch* sub-epoch (22% in F5 and 20% in F1). These two neuronal classes were not found to be neither clustered in particular sub-regions of the explored F5 and F1 cortices nor recorded at different laminar depths.

Figures 4 and 5 show single-neuron examples of the most significant categories. Spike density plots and respective rasters are aligned to the instant at which the hand touched the door handle and describe the single-unit activity during the whole grasping period (first 1500 ms in the trial). For completeness, plots in Figure 5C also include the subsequent food-grasping neuronal response, not examined in the current work. The most relevant effects of light on the grasping activity of F5 and of F1 neurons are illustrated by single-unit examples in Figure 4. Full vision of the ongoing action made these neurons discharge more intensively, compared to the full dark condition, either during the hand shaping phase of grasping (Fig. 4A), or at the contact time between the hand and the door handle (Fig. 4B) or throughout all *epoch 2*, including the very final phase of grasping (Fig. 4C). It is worth noting that these light-induced modulations were mainly expressed as additive effects to the activity recorded in the dark; indeed, the decaying part of the discharge profile of both F5 and F1 units in Figure 4A overlapped in the two conditions and so did

the ascending and descending phases of the grasping activity of the other single-neuron examples in Figure 4.

In contrast, the modulation of activity of neurons shown in Figure 5A was of a rather different kind; these units exemplify the firing behavior of a large fraction of neurons showing a significant $D>L$ effect which was actually the result of a more prolonged *post-touch* D -related response, likely associated with hand tactile/proprioceptive adjustments after the monkey's hand reached the handle under full dark conditions. In contrast, the response recorded in the L condition rapidly decayed after touch. The same observation holds for neurons shown in Figure 5B, displaying an overall more spread-out grasping activity in the D than in the L condition (with no difference at the peak activity). Single neurons in Figure 5C were largely represented both in F5 (16%) and F1 (23%) and showed a clear rightward temporal shift in the grasping response recorded in the dark, compared to that observed in the light. This was particularly evident at the discharge peak and resembled that often recorded during the following grasping of the food (see the last 1500 ms of the plots in Fig. 5C). Statistical analysis run on these neurons returned a $L>D$ (or, to a lesser extent, $D>L$) effect in the *pre-touch* sub-epoch followed by the reverse modulation in the *post-touch* sub-epoch (see “*Spurious*” entry in Table 2). Since we were mainly interested in identifying neurons showing a true L -related potentiation (amplitude increase) of motor activity and one can hypothesize that the timing difference just described might be strictly related to a difference in D/L hand kinematics, neurons of this kind were considered as a separate class, thus not influencing neither the number of cells showing a *pre-touch* $L>D$ modulation, nor the group displaying higher activity in the dark during the *post-touch* sub-epoch.

Pre-touch light-responsive neurons

Of all the cells that were light-responsive in the different temporal phases of grasping, the neuronal subset discharging more in L than D condition during the *pre-touch* sub-epoch was the

largest one (see Tab. 2). This result is of remarkable interest for the purpose of the current work, since it suggests that, although visual information on the ongoing movement was continuously available in the *L* condition, the activity of grasping neurons was particularly modulated in the period when the pre-shaping of the hand for grasping was taking place. In the following paragraphs this particular class of cells will be analyzed in detail.

Pre-touch L>D modulation had similar latency and intensity in areas F5 and F1. Figure 6A shows the time course of normalized *L* and *D* average population activity of *pre-touch* light-responsive cells in areas F5 and F1. If one considers the latency of the light-dependent effect, the two populations did not show any substantial difference. In both areas, *L* and *D* curves became significantly different (two-tail paired *Student's t-test*, 5% alpha level) 270 ms before handle touch. This result was also confirmed by the time to half-maximum divergence in activity computed on the normalized mean firing rate difference between the two conditions in the sliding 100-ms window (see *Methods*). This method returned a peak of *L* vs. *D* discharge difference in the bin centered at 80 ms prior to touch in both areas, with the half-value of this peak achieved by F5 and F1 neurons at 210 and 190 ms before touch, respectively.

In addition to the temporal properties of the effect, the intensity of light-responsiveness displayed by the two neuronal groups was almost comparable. This was measured over time by computing the population mean ROC area for the two conditions on every 100-ms bin. Figure 6B shows that F5 and F1 light-responsiveness developed in a similar way around the handle grasping period, though F1 selectivity was overall stronger. The distribution of *pre-touch* ROC area values across neurons (Fig. 6C) confirmed that, although slightly higher in F1 than in F5 (ROC area was higher than 0.7 for 88% of neurons in F1 and 63% of neurons in F5), light-sensitivity during hand shaping was similar in the two areas.

Unlike F1 neurons, F5 neurons showed significantly different response profiles under light and dark conditions. If no differences between F5 and F1 populations were present as for latency and intensity of the *L*-dependent modulation, neurons of the two areas differed in regard to the specific discharge profile displayed during the *L* and *D* conditions. Whereas the F1 population showed *L* and *D* response profiles growing up and reaching their peak of response almost in parallel, in area F5 the slope of *L* and *D* responses clearly differed. Figure 6D shows the average temporal peak and latency of the F5 and F1 response during the two conditions. The mean peak and latency times of the F5 neuronal responses were significantly shorter in the *L* condition than in the *D* condition (two-tail paired *Student's t-test*, 5% alpha level). Overall, F5 *pre-touch L*-sensitive neurons peaked much earlier in full light (-94 ± 25 ms, mean \pm S.E.M.), than in full dark (-47 ± 29 ms) ($t(23) = 2.3$, $P = 0.03$). They also displayed a much faster ramping activity to the peak in full light (-135 ± 27 ms) than in full dark (-81 ± 30 ms) ($t(23) = 2.7$, $P = 0.01$), as revealed by the time-to-half-the-maximum parameter. In contrast, F1 population showed no timing difference in the grasping activity between the two conditions, neither at the latency (*L*: -96 ± 23 ms; *D*: -87 ± 39 ms, $t(15) = 0.4$, n.s.), nor at the peak (*L*: -39 ± 26 ms; *D*: -38 ± 41 ms, $t(15) = 0.05$, n.s.) of discharge.

In addition, a linear regression function interpolating the activity of each cell of F5 and F1 *pre-touch L*-selective populations in a 300-ms window prior to touch (i.e., going from -300 to 0 ms and representing the most significant portion of the *pre-touch* response profile) was computed for *L* and *D* conditions. Neurons showing a negative slope regression parameter *m* (i.e., the first derivative) in both conditions, thus characterized by a substantially different response profile with respect to the other neurons in the population, were discarded from the analysis. Whereas in the F1 population ($n = 13$) the slope regression parameter of the ramping activities in *L* (median $m = 63.7^\circ$, Inter-Quartile Range, IQR = 11.4°) and *D* ($m = 49.4^\circ$, IQR = 16.4°) conditions was comparable (*Wilcoxon signed ranks test*, $W^+ = 1.6$, n.s.), in the F5 population ($n = 20$) it significantly changed (*L*: $m = 57.1^\circ$, IQR = 33.8° ; *D*: $m = 40^\circ$, IQR = 31.7° ; $W^+ = 2.7$, $P = 0.006$). Figure 6E shows fitting

line plots for the *D* and *L pre-touch* response profiles of F5 and F1 *L*-selective neurons both at population (left plots) and single-unit (right plots) level. Whereas for the majority of F5 neurons the slope of the *pre-touch* response was appreciably steeper in the *L* than in the *D* condition, for most of the F1 neurons it did not significantly differ in the two conditions (Fig. 6F).

Importantly, none of the F5 and F1 neurons which were *L*-responsive in either of the other considered sub-epochs displayed such a significant timing difference between the *L* and *D* response profiles, indicating that this result was highly specific for the *pre-touch L*-selective neuronal population recorded from area F5.

Taken together, these results indicate that the effect of light over the activity of F5 *pre-touch L*-responsive neurons, in contrast to that of F1 neurons, mainly consisted in a temporal gain of the *L*-related response over the *D*-related one. This was achieved through a faster increase of the *pre-touch* activity when the monkey could observe its own hand during the pre-shaping phase of grasping, compared to when it could not. In addition, there is some indication for a functional interplay between area F5 and area F1. The motor discharge of the F1 *pre-touch* neurons in the *L* condition was consistently, though not significantly (*Student's t*-test, 5% alpha level), delayed (39 and at the latency and 55 ms at the peak) with respect to that of the F5 population, suggesting a transfer of visual information from premotor to primary motor cortex neurons for correct grasping execution.

Were light-responsive neurons also modulated by transient visual feedback?

We analyzed whether neurons modulated by light (both positively and negatively; n=104, 61% of F5 neurons; n=70, 54% of F1 neurons; see Tab. 2) were also sensitive to the transient visual feedback provided in the two *flash* conditions. A running *t*-test (see *Methods*), contrasting *D* with either of the two flash conditions was performed on the activity of each neuron during *epoch 2*.

We found that 54 F5 neurons (32% of the F5 recorded sample) and 42 F1 neurons (25% of the F1 recorded sample), all light-responsive ($L>D$ or $D<L$), were also modulated by flashes. In particular, 19% of F5 neurons, in addition to showing a $L>D$ modulation, also displayed a significant increase of response to either (PT , 5%; T , 9%) or both (5%) flash conditions with respect to D . Similarly, 14% of F1 neurons showed a $L>D$ effect and discharged more during PT (6%), T (4%) or both (4%) flash conditions than during D .

A relevant fraction of the $L>D$ neurons modulated by flashes was represented by *pre-touch* L -selective neurons described above (6% in area F5 and 5% in area F1). Specifically, 11 out of the 24 F5 *pre-touch* L -selective neurons (46%) discharged significantly more in PT flash (17%), T flash (25%) or in both flash conditions (4%), than in the dark. *Pre-touch* light-selective neurons in area F1 that were sensitive to transient visual feedback (36%) were equally modulated by PT flash (12%), T flash (12%) or both flashes (12%). These flash-related responses were generally observed in grasping periods congruent with flash presentation, namely during *pre-touch* sub-epoch for neurons responsive to PT flash and at *touch* for neurons selectively modulated by T flash.

As far as $D>L$ modulations are concerned, 13% of F5 neurons showed a significant decrease of firing rate in response to L and either PT (8%), T (3%) or both flashes (2%), compared to D condition and 11% of F1 neurons behaved similarly, discharging significantly less than D in L and either PT (3%), T (5%) or both (3%) flash conditions.

Hence, most of the $L>D$ and $D>L$ modulated neurons responded to flash presentation with higher or lower firing rates with respect to D , congruently with the response recorded in the L condition during the same grasping epoch. In some cases (2% of neurons in both areas), the activity during flash conditions significantly exceeded that observed in full light, indicating that a transient visual information, delivered during significant grasping phases, was effective in modulating the firing of these neurons much more than the visual feedback available during the whole hand movement.

Only a small amount of those neurons that were not modulated by the full vision of the own grasping movement, were found to be responsive to light flashes. Five percent of neurons in both areas showed indeed a significant enhancement of their response to either flash condition compared to both *L* and *D*. Three percent and 2% of non-modulated neurons respectively recorded from area F5 and area F1 showed a significantly decreased flash-related response.

PT flash vs. T flash: selectivity for specific transient visual feedbacks

The above reported results suggest that several grasping neurons influenced in their discharge by the continuous availability of the visual feedback with respect to darkness, were also modulated when such visual information was just briefly available. To analyze more in depth this modulation, but to get rid at the same time of any unspecific effect carried by light flash stimuli, we took into account only those neurons showing a modulation of their response during either flash. This was done by directly contrasting, through a running *t-test* analysis, the single-neuron responses to *PT flash* with those to *T flash* (see *Methods*). Neurons exhibiting a significant difference in activity between the two flash conditions were identified as flash-selective and their behavior was then thoroughly studied at the population level and in relation to the *D* and *L* conditions as well.

This running *t-test* analysis revealed a large portion of both F5 (48%) and F1 (43%) neurons that, within *epoch 2*, were selectively modulated by the transitory vision of the own ongoing action. The direction of the modulation was the following: neurons showing more activity during *PT flash* than during *T flash* condition were 19% in area F5 and 22% in area F1. Neurons showing the opposite behavior (more activity in response to *T flash* than to *PT flash*) were 29% in area F5 and 21% in area F1 (see Tab. 2). A small percentage of neurons (4% in area F5 and 1% in area F1) were responsive to both flashes (obviously in different time windows) and were not taken into further consideration.

The flash selectivity was time-locked to the time of flash occurrence (*pre-touch/touch* sub-epoch for *PT flash* selectivity and *touch/post-touch* sub-epoch for *T flash* selectivity) for most of the flash-selective neurons in both areas: 12% (*PT flash*) and 22% (*T flash*) in area F5 and 12% (*PT flash*) and 17% (*T flash*) in area F1. The remaining *PT flash*- and *T flash*-responsive neurons of both areas exhibited flash selectivity that was either delayed (i.e., *PT flash*-selectivity present in the *post-touch* sub-epoch) or anticipated (i.e., *T flash*-selectivity evident in the *pre-touch* sub-epoch) with respect to the time of flash delivery. These neurons likely represented the effect of flash-related predictive and/or inhibitory mechanisms.

Figure 7 shows examples of individual flash-responsive F5 and F1 neurons.

From this preliminary analysis we gathered that the percentage of flash-selective neurons was almost the same in the two recorded areas. Further analyses were then performed to extensively compare flash-related modulations in the two areas.

Latency of F5 and F1 flash-selectivity was consistent with the specific grasping time at which the flashes were delivered. Figure 8 shows flash-related activity, expressed in terms of average profile of discharge, for F5 and F1 *PT flash*- (A) and *T flash*-selective (B) populations. As resulting from the running *t-test* analysis, the traces referring to the activity in the two flash conditions began diverging much earlier in the *PT flash* than in the *T flash*-selective neuronal groups in both areas. Indeed, *PT flash*-responsive neurons started firing significantly higher in the *PT flash* condition than in the *T flash* condition at the 100-ms bin centered at -430 ms (F5) and -410 ms (F1) before handle touch. In contrast, F5 and F1 *T flash*-selective neurons started displaying their selectivity respectively at -170 and -150 ms. Note that both *PT flash*- and *T flash*-selective neurons might display some predictive behavior, discharging overall well in advance with respect to the instant of flash occurrence (details concerning the time of *PT flash* presentation are reported in

Table 1). These anticipatory flash-related responses of the neurons were likely dependent on the blocked design of the experiment.

The difference in latency of the two flash-related modulations was confirmed by computing the time to half-maximum divergence in activity between the two flash conditions, which was shorter for the *PT flash*-responsive neurons (F5, -210 ms; F1, -170 ms) than for those specifically sensitive to *T flash* (F5, -130 ms; F1, -130 ms). A closer examination of the time-course of the modulations, as processed by the ROC analysis, revealed flash-related complementary responses in area F5 (Fig. 8C, left). The time course of *PT flash*-related selectivity was characterized by a gradual increase during the pre-shaping phase of grasping, followed by a quite fast decay immediately after touch. Conversely, *T flash*-related selectivity increased rapidly before touch, reached the highest value at the hand-handle contact and declined slowly in the *post-touch* sub-epoch, persisting throughout the final phase of grasping. According to the running *t-test* analysis, the *PT flash* effect became manifest 260 ms earlier than the *T flash* effect and disappeared 200 ms earlier (the *PT* and *T flash* last significant bins were respectively centered at 190 ms and 390 ms after touch, see Fig. 8A-B for F5 populations). The onsets of *PT* and *T flash* signals in area F1 showed a time shift (about 200 ms) comparable to that observed in the activity of F5 flash-responsive neurons (Fig. 8C, right). However, in contrast to F5, F1 *T flash* effect was more temporally locked to the handle touch instant, decaying 60 ms earlier than the *PT flash* effect (see Fig. 8A-B for F1 populations).

Flash-related responses were stronger in area F5 than in area F1. Flash-related information conveyed by F5 neurons within *epoch 2* was overall higher than that of F1 neurons, especially considering *T flash* selectivity. This result emerges after comparing the time course of ROC values of the flash-responsive groups recorded from the two brain regions (Fig. 8D).

PT flash-selectivity in F5 was overlapping in strength that of F1 during the pre-movement period (*epoch 1*); then, around 250 ms before handle touch, it reached a higher level which was maintained for all the *pre-touch* sub-epoch and till about 100 ms after touch. Accordingly, the area under the ROC curve was inferior to 0.3 (indexing strong *PT flash*-related signal) for 44% of F5 *PT flash*-selective neurons during both *pre-touch* and *post-touch* sub-epochs. For *PT flash*-selective neurons in area F1 this percentage was lower (*pre-touch* sub-epoch, 34%; *post-touch* sub-epoch, 38%) (Fig. 8E).

Even more evidently, *T flash*-selectivity in F5 started increasing approximately at the same time (-250 ms) as the one observed in F1, but diverged considerably from it around 100 ms before the contact of the hand with the door handle. This ROC area difference persisted through all *touch* and *post-touch* sub-epochs, decaying only after the end of the grasping movement (around 450 ms after touch). Area F5 conveyed indeed more *T flash*-related information than area F1, both during *pre-touch* (ROC area higher than 0.7 for 39% of F5 *T flash*-selective neurons and 26% of F1 *T flash*-selective neurons) and *post-touch* (F5, 41%; F1, 33%) sub-epochs (Fig. 8E).

Figure 9 shows the average activity of each flash-selective population in all four experimental conditions along the trial. From these population plots, the following considerations can be drawn:

- a) Response profiles of area F5 differed from those of area F1, varying a lot across conditions.
- b) F5 and F1 neurons responding to specific transient visual information appeared to be not particularly responsive during grasping performed under continuous visual feedback conditions.
- c) Unlike F1 neurons, F5 flash-selective neurons seemed to display the maximal response to the transient visual feedback for which they expressed selectivity.

In the next paragraphs, these aspects will be thoroughly examined with particular emphasis given to differences between the two recorded areas.

a) The same visual feedback delivered at specific different phases of grasping differentially modulated F5 neurons but not F1 neurons. First of all, we analyzed the response profile displayed by F5 and F1 flash-selective populations, and we used the temporal dispersion (Inter-Quartile Range, IQR, a robust estimate of data dispersion) of the discharge peaks of the neurons included in each population as a measure for that (see Tab. 3 and inset box plots in Fig. 9). Flash-selective cells of area F5 exhibited, on average, a rather spread-out grasping-related response (IQR = 144 ms), as opposed to the more compact one of the F1 flash-selective neurons (IQR = 72 ms). A dispersion test (*Ansari-Bradley test*, 5% alpha level) revealed that the temporal variability in the discharge peaks was significantly different in the two areas ($W^* = 5.8$, $P < 0.0001$), particularly when contrasting the F5 and F1 *PT flash*-selective populations (IQR = 161 ms and 56 ms, respectively; $W^* = 7.3$, $P < 0.0001$). Conversely, non-flash-responsive neurons in the two areas displayed comparable firing dispersion (F5 IQR = 125 ms; F1 IQR = 123 ms; $W^* = 1.1$, n.s.). More importantly, the average response profile of F5 flash-selective neurons in the different conditions specifically varied according to the flash condition for which they expressed selectivity (see inset box plots for area F5, Fig. 9A-B). In particular, the firing dispersion shown by F5 *PT flash*-responsive neurons in the *PT flash* condition (IQR = 214 ms) was significantly greater than that calculated in the same neurons for the *D* (IQR = 120 ms; $W^* = 2.1$, $P = 0.04$) and *T flash* (IQR = 78 ms; $W^* = 2.9$, $P = 0.003$) conditions. On the contrary, the discharge peaks of F5 *T flash*-selective neurons were consistently less dispersed in the *T flash* condition (IQR = 114 ms) than in the *D* (IQR = 199 ms; $W^* = 1.9$, $P = 0.05$) and *PT flash* conditions (IQR = 144 ms; $W^* = 1.1$, n.s.). Interestingly, in both *PT* and *T flash*-responsive populations, the behavior observed during the flash condition for which the neurons were selective approached that assumed in the *L* condition (IQR = 199 ms and IQR = 112 ms,

respectively), which, in turn, differed substantially from that measured in the *D* condition (for details, see Tab. 3).

Opposite to what observed in area F5, the average response distribution of F1 neurons in the flash condition in which they conveyed more information was not significantly different from that of the *D* condition. Independently of the specific F1 flash-responsive population they were assigned to, these neurons showed firing peaks with similar temporal dispersion in the *PT flash*, *T flash* and *D* conditions. In all three conditions, they increased their discharge variability with respect to the *L* condition (see inset box plots for area F1, Fig. 9A-B and Tab. 3).

These results suggest that the same transient visual feedback, if delivered at meaningfully different phases of grasping, produced different effects on the activity of F5 neurons within a specific selective population, including modulating their firing dispersion in a way that is coherent to the behavior observed for the same neurons when continuous visual feedback was available.

b) F5 and F1 flash-selective neurons were overall not light-responsive. The majority of both F5 and F1 flash-selective neurons did not show any significant light responsiveness. Only a small fraction of neurons responsive to *PT flash* (2% in both F5 and F1 area) and to *T flash* (6% in F5 and 5% in F1) displayed firing rates significantly higher in *L* than in *D*, and mainly during the *pre-touch* sub-epoch (see “*Intersection with L>D neurons*” in Tab. 2). In fact, flash-selective neurons represented relatively heterogeneous populations with regard to the behavior they expressed in *L* and *D* conditions, with a relevant portion of them pertaining to (i) non-selective neurons (10% in F5 and 6% in F1; e.g., F5 neuron #013-1, Fig. 7B), (ii) neurons discharging more during grasping in dark than in light (21% in F5 and 12% in F1; e.g., F5 neuron #045-2, Fig. 7A, showing a *D>L* modulation in both sub-epochs of *epoch 2* and F5 neuron #016-3, Fig. 7B, displaying a *post-touch D>L* effect), and (iii) neurons displaying “*spurious*” effects, due to a temporal shift between *L*- and *D*-related response profiles (9% in F5 and 18% in F1; e.g., neurons #033-1, #223-1 and #165-1, Fig.

7). Note that the majority of flash-selective neurons in F5 showed a $D > L$ modulation, whereas most of F1 flash-responsive neurons displayed a “*spurious*” effect, which well explains the different response profile in the L condition compared to the other dark conditions in the F1 population plots (Fig. 9). These findings suggest that flash-selective neurons represented a quite different population with respect to that formed by light-responsive neurons; indeed, they either showed decreased responses or were not affected by the fact of performing grasping in light.

c) Unlike F1 neurons, F5 flash-selective neurons displayed the maximal response to the transient visual feedback for which they expressed selectivity. To better evaluate flash selectivity of these populations, we compared the single-neuron response to the preferred flash with that recorded during D and L conditions. According to the running *t-test* analysis, we found that the majority of flash-selective neurons in area F5 (52/81, 64%) displayed a significantly higher activity in the flash condition for which they expressed selectivity than in the D condition. For most of these neurons (46/81, 57%), the flash-related response was even significantly stronger than the L -related one. A smaller amount of flash-selective neurons in area F1 (22/56, 39%) showed the same kind of modulation, with the response to the preferred flash being higher than that to both D and L in 29% of cases.

Similar analyses were performed at the population level. Two one-way ANOVAs with *condition* (D , L , PT flash and T flash) as factor were run on the response of each F5 and F1 flash-responsive population during both *pre-touch* and *post-touch* sub-epochs. Figure 10 (A, B) illustrates the main statistical results: PT flash-responsive neurons in area F5 showed the strongest response to PT flash during *pre-touch* sub-epoch (Fig. 10A, left): firing rates recorded during the other experimental conditions were significantly lower ($F[3, 93] = 5.51$, $P = 0.01$; $P < 0.05$, LSD post-hoc tests) and, interestingly, response to the other flash condition (T flash) was decreased with respect to the activity recorded during the D condition ($t(31) = 2.05$, $P < 0.05$). In contrast, F1 PT flash-

selective population displayed no difference in the *pre-touch* activity among the four conditions ($F[3, 84] = 1.98$, n.s.) (Fig. 10A, right). During *post-touch* sub-epoch, *PT flash*-selective populations behaved similarly in the two areas: *PT flash*-related response was stronger than *T flash*- ($P < 0.001$) and *L*-related ($P < 0.0001$) ones, though not different from the activity in the dark (F5: $t(31) = 1.73$, n.s.; F1: $t(28) = 0.76$, n.s.) (Fig. 10A).

T flash-responsive neurons in area F5 showed the highest activity in response to *T flash* both during *pre-touch* ($F[3, 144] = 6.42$, $P = 0.0004$, pairwise LSD comparisons with other conditions significant at $P < 0.05$) and *post-touch* ($F[3, 144] = 15.9$, $P = 0.000001$, comparisons with other conditions significant at $P < 0.0001$) sub-epochs (Fig. 10B, left). On the contrary, F1 neurons selective for *T flash* only displayed a significant difference in activity between the two flash conditions in the *post-touch* sub-epoch ($F[3, 78] = 3.62$, $P = 0.02$; $t(26) = 3.06$, $P = 0.005$). F1 response to *T flash* was not significantly increased with respect to neither that recorded in the *D* ($t(26) = 0.15$, n.s.) nor that observed in the *L* ($t(26) = 0.17$, n.s.) condition. In addition, no significant *T flash*-related modulation was evident in the activity of these F1 neurons in the *pre-touch* sub-epoch ($F[3, 78] = 2.11$, n.s.) (Fig. 10B, right).

Given the above-described differences in the response profiles of the F5 and F1 populations, as determined by the variability of the neurons' discharge peaks (higher in the F5 than in the F1 flash-selective populations), an additional measure of the strength of the flash-related response was obtained by comparing the peak firing rates of the neurons assigned to each population in the four conditions. The main results of the one-way (*condition*) repeated-measure ANOVA are summarized in Figure 10 (C, D). For completion, differences among conditions assessed at the time to half-maximum activity (referred to as the latency) of the neurons are also reported for each population. As far as area F5 is concerned, this analysis emphasized the ANOVA results obtained averaging activity in *pre-touch* and *post-touch* sub-epochs (Fig. 10C, left). The discharge peak in the preferred flash condition was clearly the highest among conditions for both *PT flash*- ($F[3, 93] = 3.65$, $P =$

0.02; $P < 0.02$, LSD post-hoc tests) and *T flash*-selective ($F[3, 144] = 10.54$, $P = 0.0001$; $P < 0.05$, LSD post-hoc tests) F5 populations. In addition, this analysis revealed a significant *L>PT flash* effect in the mean latency ($t(48) = 2.4$, $P = 0.02$) and peak ($t(48) = 2.4$, $P = 0.02$) activity of the *T flash*-selective neurons, stressing the strong *T flash* information carried by this population, partially due to the suppression of the *PT flash*-related signal (Fig. 10D, left). On the contrary, the F1 flash-responsive groups did not show any distinct peak predominance of the specific preferred flash condition over all the other conditions, especially if considering *PT flash*-selective neurons (Fig. 10C, right). *Touch flash* maximum activity of F1 *T flash*-responsive neurons was higher than that of *PT flash* ($F[3, 78] = 3.002$, $P = 0.04$; $t(26) = 3.2$, $P = 0.004$) and *D* conditions ($t(26) = 2.9$, $P = 0.007$), but not significantly different from that measured in the *L* condition ($t(26) = 0.64$, n.s.) (Fig. 10D, right), as it was in the case of F5 *T flash*-selective population.

To summarize the results obtained with the last described analyses, transient visual information fed back from a specific phase (either hand pre-shaping or contact between the hand and the to-be-grasped object) of the own ongoing grasping action strongly influenced the response of F5 neurons in many ways. Indeed, unlike F1 neurons, (i) F5 neurons within a specific flash-selective population rearranged their firing temporal dispersion as a function of the specific visual feedback received (see Fig. 9 and Tab. 3). (ii) F5 flash-selective neurons significantly increased the response to the preferred transient visual information, compared to all the other experimental conditions, including full light. This strong flash-selectivity was evident both when looking at the average activity of the neurons in the *pre-touch* and *post-touch* sub-epochs of the different conditions and at the discharge peaks of the neurons in the four conditions (Fig. 10). (iii) F5 neurons conveyed flash-related signals that, in addition to being predominantly present in the sub-epoch during which the preferred transient information was delivered, also persisted all through the grasping epoch (see Fig. 9 and Fig. 10).

DISCUSSION

The present study investigated whether primary motor area F1 and ventral premotor area F5 contain visuomotor neurons which do not show any visual response associated to the observation of 3D objects (canonical neurons) or to actions performed by other individuals (mirror neurons), but rather, are sensitive to the observation of the monkey's own ongoing grasping movement. These neurons, which we proved to be present, exhibit visuomotor properties that are common to both purely motor and mirror neurons, hence allowing new speculations on the critical role of online visual information during grasping execution and on the nature/genesis of the mirror neurons' visual response. Indeed, both in area F5 and in area F1 a significant percentage of neurons modulated their grasping-related activity as a function of the duration (continuous or transient) and of the grasping phase (hand pre-shaping- or hand-object contact) during which the visual feedback was delivered. The effects observed in these two motor areas present some important differences, suggesting a distinct functional contribution of the ventral premotor and primary motor cortices to the analysis of motor-relevant visual feedback. These are the main results: (i) The neuronal response during grasping performed in light is anticipated in area F5 with respect to area F1; (ii) F5 neurons are more sensitive than F1 neurons to specific transient visual information received during grasping.

Both F5 and F1 neurons potentiate their motor activity during hand shaping in light, but F5 neurons show a faster increase of light-related responses

By comparing the grasping-related activity of the neurons during light and dark conditions, a variety of neuronal categories could be distinguished, both in area F5 and in area F1, depending on the time course of their modulation. The main modulation was mostly due to a more prolonged activity when the monkey was grasping in dark, with respect to full vision condition. Indeed, a large

amount of neurons in both areas displaying overlapping pre-touch responses in light and dark, differentiated their response in the post-touch phase, mainly because of the contrast between the rapid firing decay during light and the more long-lasting activity recorded in dark. This neuronal behavior, that statistically produced a post-touch $D > L$ effect, was rather likely related to finger posture corrections ensuing tactile/proprioceptive feedbacks from the hand-object contact in the dark, as we observed in some pilot kinematics experiments. However, being the aim of our study the detection of neurons sensitive to the vision of the own grasping hand, we concentrated on neurons that, in full light, potentiated their discharge.

These neurons, representing a relevant proportion (22%) of both our F5 and F1 samples, resemble those previously described in area AIP (Murata et al. 2000; Sakata et al. 1995) which have been suggested to play some role in encoding the pattern of hand movements during handgrip formation. The light-sensitive neurons reported in the present work, as well as the AIP *nonobject-type* neurons, modulated their activity as a function of the fact that the monkey grasped under light or dark conditions. Moreover, they did not respond to object presentation, as shown by the naturalistic testing and by the absence of any response to the mere observation of the to-be-grasped door handle before movement onset during the formal task.

Particularly relevant is the result that, although visual information on the own ongoing action was continuously achievable in the light condition, the activity of the majority of the recorded neurons was mainly affected by it during hand pre-shaping and landing onto the object, i.e., when visual feedback mostly matters. In fact, among light-selective neurons, those specifically enhancing their activity in the period preceding the contact with the object, were the most represented ones, both in area F5 (14%) and in area F1 (13%).

This finding can be subjected to more than one specific interpretation, including, first of all, the critical influence that the online visual feedback may exert on grasping kinematics. Indeed, although the experimental apparatus was designed so as to minimize at best hand movement

variations between light and dark conditions (the position of the to-be-grasped object was made detectable also in the dark), analyses carried out on the kinematic trajectories recorded during the behavioral experiment revealed some crucial, though subtle, differences between the two conditions. As reported in literature (Churchill et al. 2000; Schettino et al. 2003; Winges et al. 2003), an increase in the duration of the deceleration phase and of finger closing was found when grasping was performed in the dark. Moreover, maximum grip aperture became wider, indexing that, without vision, the monkey tended to increase the grip size safety margin for grasping the door handle successfully (Rand et al. 2007).

Close inspection of the firing properties of *pre-touch* light-selective neurons revealed an important timing difference characterizing the grasping-related response of the F5 population in the light and dark conditions. When the reach-to-grasp task was performed under constant online visual feedback, the latency and peak times of the discharge of these neurons were significantly shorter than those observed during the execution of the same task in absence of any visual information. Thus, F5 neurons showed a fast raise of the activity to the peak in full light, as opposed to the slow, gradually increasing firing rates exhibited during the *pre-touch* phase in the dark. In addition, F1 neurons showed a pre-touch light-related response that was delayed in time and slightly strengthened in amplitude with respect to that of F5 neurons, suggesting a functional interplay between the two areas that could explain the kinematic differences observed between the light and dark conditions. These light-dependent timing effects indeed could well correlate with the faster grasping approach adopted by the monkey under continuous visual feedback conditions, mainly involving arm velocity during reaching. The hypothesis that these data mostly relate to movement kinematics is also supported by many neurons that markedly anticipated their motor response under full light condition (16% in F5 and 23% in F1) with respect to dark condition. Even more generally, the finding that a higher percentage of neurons were strengthening (31%, including both areas),

rather than diminishing (13%), their activity in the most critical period of the grasping movement (*pre-touch/touch* period) during light, appears to favor this interpretation.

It is thus arguable that, the pre-touch light-selective cells described here form a neuronal sub-circuit, involving both F5 and AIP areas, that is specifically relevant to visual feedback-based adjustments of the handgrip during movement. More direct evidence is however required to support this hypothesis, based on systematic studies of the correlation between hand kinematics and neuronal activity.

Another possible account for the light-modulated grasping responses of these neurons is that they may represent one of the many instances of the observation-evoked motor activation that is typical of mirror neurons. Indeed, it has been demonstrated that the F5 mirror visual discharge can reflect the neuron's motor selectivity at several degrees of abstraction (di Pellegrino et al. 1992; Gallese et al. 1996; Nelissen et al. 2005). Recently, also single-neuron activity in area F1 has been shown to be similar during both execution and passive observation of a familiar motor task (Tkach et al. 2007). Interestingly, F1 neurons were found to respond to the view of a reliable surrogate of the monkey's own hand (a visual cursor projected on a screen), moving in an abstract workspace.

Also in our study, monkeys were observing their own, as opposed to others' (co-specific or human) hand grasping; however, differently from the study mentioned above, the observed movements were actively performed. In this particular case, the action which the cells contribute to generate, perfectly matches the one potentially evoking a neuronal response in the same cells through observation. Hence, because mapped on the same active movement, the discharge elicited by observation is not easily dissociable from the one related to execution and the increase in activity shown by the light-responsive neurons during the light condition with respect to the dark condition, cannot be univocally interpreted as a neuronal activation purely induced by the vision of the own grasping movement.

Hence, given these last remarks and the evidences reported above suggesting a possible correlation between the activity of these neurons and hand kinematics, we conclude that, within the light/dark comparison, observation-evoked responses cannot be dissociated from modulations due to changes in movement execution.

Both F5 and F1 neurons selectively respond to motor-relevant transient visual feedbacks, but area F5 shows a higher specificity for the type of grasping-related information they bring

To exclude any influence of kinematics on the observation-dependent responses of the recorded neurons, two light flash conditions were introduced in our experiment. No substantial hand kinematic difference was indeed found between the two flash and the full dark conditions. Conversely, several recorded neurons displayed specific selectivity for either of the two light flash conditions, suggesting that the behavioral paradigm succeeded in revealing neuronal effects dependent on the vision of brief fragments of the own grasping action. Specifically, a large number of both F5 (48%) and F1 (43%) cells statistically showed a difference in the grasping-related activity, that was dependent on whether transient visual information was fed back from the handgrip configuration period or hand-object contact instant. Importantly, the latency of flash-selectivity displayed by these neuronal populations tightly reflected the point in time of flash occurrence, that is, earlier in the trial when visual feedback was given during pre-shaping, with respect to when it was delivered at the handle touch. One possible criticism may be that the found neuronal modulations rather depended on an arousal effect, time-locked to flash presentation. Our results show that this was not the case.

First, since the analysis consisted in directly contrasting the activity displayed by the same cell in the two flash conditions, all neurons showing a significant response to both flashes during the grasping period (that could be indicative of an arousal reaction in the monkey) were not taken into consideration. Second, the flash selectivity of the neurons did not generally emerge

immediately after one given flash was delivered (that would suggest the existence of a strict temporal relationship between the arrival of a transitory visual event and the onset of the neuronal response); rather, it appeared at different times around flash presentation and, in some cases, even in advance of it, meaning that neurons were not only online signaling, but also “expecting”, the availability of the flashed motor-relevant visual information (the experiment was performed in blocks). Moreover, particularly in area F5, cells continued conveying this information well after flash offset, denoting that for the animal engaged in performing the grasping movement, this was in some way a meaningful event, rather than simply a startling stimulus.

It is also to note that the degree of overlap between any of the light-sensitive neuronal classes and flash-selective neurons was poor in both areas, supporting the assumption that the neuronal modulations due to continuous vision of the movement were, in all probability, of a different kind with respect to those observed during brief illumination of the motor action scene. Thus, since kinematics and arousal are not to be considered as important confounding variables, the hypothesis that flash-related modulations represented the selective response of the neurons to the observation by the monkey of its own ongoing grasping at specific time windows (when the view of the movement was briefly allowed), can be strongly put forward.

The fact that observation-evoked responses were recorded also in the primary motor cortex is not surprising. Significant changes in M1 cortical activity during action observation have been reported by several human studies, using different techniques (Caetano et al. 2007; Cheng et al. 2007; Fadiga et al. 1995; Muthukumaraswamy and Johnson 2004). In addition, Tkach et al. (2007) have tackled the issue of observation-related M1 activation at the single-unit level, describing neuronal discharge and local field potentials associated with the passive view of one's own movements.

However, the detailed analysis of the visually-modulated activity of the neurons recorded in the present research revealed that F1 flash-evoked neuronal effects differed from those found in F5

as far as some critical features are concerned. First, the level of flash selectivity, defined as the relative difference in the neuron's grasping activity between the two flash conditions, was lower in area F1 than in area F5. More relevant, the signal related to transient action observation brought by F1 neurons was in general not significantly stronger than the one they showed under continuous visual feedback conditions. In contrast, F5 neurons exhibited the maximal discharge in response to the delivery of the light flash which they were sensitive for, both at the peak and during the relevant grasping epoch, suggesting that the visual information conveyed by the brief enlightenment of the hand movement was extremely efficient in strengthening the ongoing motor activity of these neurons.

Moreover, population analyses showed that the pattern of activation of F5 neurons was highly specific for the type of visual feedback received. In particular, the transient observation by the animal of its own movement during the hand pre-shaping phase of grasping, besides augmenting considerably the motor response of the neurons, specifically increased the temporal dispersion of their discharge peaks compared to the dark condition. Conversely, the F5 population selectively active in the final period of grasping, when the monkey could briefly look at its own hand contacting the door handle, displayed a more temporally compact distribution of the neurons' firing peaks. Interestingly, flash-selective populations modulated their firing dispersion in a way that was consistent to the behavior observed in the same neurons during full vision of the movement. Hence, the same visual stimulus, presented at different critical stages of the grasping action, differentially affected F5 neuronal response. This suggests that the possibility of transitorily accessing the view of meaningful bits of the own ongoing movement, online specifically reinforced the motor program used to execute that particular action.

The computational study of motor control has provided important working principles concerning the relationship between sensory signals and motor commands. It is currently thought that the motor system is governed by two main internal processing models, which control the causal

link between actions and their consequences (Wolpert and Ghahramani 2000). Inverse models implement the transformation from the desired consequences (i.e., the goal) of an action to the motor commands necessary to execute that action. Any form of motor pre-programming, as in the case of the present reach-to-grasp task, implicitly involves this inverse relationship. Forward models, instead, monitor the state of the current motor commands by continuously predicting the consequences of them, through sensory feedback from the periphery. Thereby, forward models can support sensorimotor control by minimizing sensory and motor noise in many ways, including integrating, invalidating or anticipating the kind of sensory inflow that constantly update predictions (Bays and Wolpert 2007; Miall 2003).

In the context of the present experiment, for instance, estimation of the state of the system could have supplemented noisy or absent visual information during grasping in full dark, or generated the appropriate adjustment signals for online grip control after, or in advance of, a visual reafference from the transient observation of the action during flash delivery. Indeed, the enhancement of motor activity in the flash-selective populations in response to the brief illumination of the grasping hand might be the result of forward predictions, intervening over the ongoing inverse sensorimotor transformation for handle grasping. In addition, the increased timing variability in the firing peaks of the neurons (measured during the brief view of the own hand before the contact with the handle) might be directly reflecting the uncertainty of estimation about the position of the hand relative to the handle and thus be related to the error signal produced to fast online re-program the posture of the fingers with respect to the target. Conversely, the more temporally compressed discharge of the neurons in response to the sight of the hand touching the handle (a grasping event that is perceptually and temporally more defined than pre-shaping and hence, more easily predictable) might be indicative of a reinforcement signal, confirming the correct forward estimation of the state of the system at that point of grasping.

Taken together, these results confirm that area F5 contains visuomotor neurons which are specifically activated by the transitory observation of meaningful phases of the own grasping movement.

Turning to the issue, initially addressed, of the nature of the visuomotor coupling at the basis of the mirror response, what then might be the role of F5 neurons showing these peculiar visuomotor properties? How can these findings be interpreted in the framework of a theory supposed to explain the development of mirror neurons? Finally, what might be the functional interplay between F5 and F1 neurons displaying observation-evoked motor responses of the kind described by our work?

Interpretational issues

It has been suggested that mirror cells, originally described in area F5, lie at a crucial interface between inverse and forward models (Carr et al. 2003; Iacoboni et al. 2005). Connections from STS to PF, and frontward to mirror neurons in F5, would represent an inverse model mapping the visual description of actions onto the motor commands that are needed to execute them. The reverse projections from F5 to PF and backward to STS would instead correspond to a forward model translating the actual motor plan into a predicted sensory representation of it. This two-way model could be responsible for the activation of mirror neurons during both action execution and observation. However, though very elegant, this scheme presents some contradictory points.

First, the predictions made by forward models are, by definition, very specific, as they are to provide the motor system with helpful information to constantly control movement outcome. On the other hand, F5 observation-related mirror responses are characterized by different levels of generality.

Second, forward models originally imply that estimations about the current state of the motor system mainly involve our own actions, whereas the mirror visual discharge has never been described as concerning first-person motor action observation.

The hyper-MOSAIC computational model developed by Wolpert et al. (2003) takes into account the former argument, proposing that multiple paired forward/inverse models act in parallel to estimate and control motor states at different hierarchical levels of abstraction. Whereas lowest levels would imply an extremely congruent matching between executed and observed actions, the highest layers would represent the behavioral goal of actions, unbounded from the specific motor effector or kinematic details of the action. Intermediate stages would progressively receive from previous layers, coding actions at increasingly more abstract levels.

However, how the lowest layers of this architecture can be neuronally generated is not yet well understood. The visuomotor neurons described in the present study, for the fact that they receive facilitatory inputs activated by the sight of specific phases of the own action, thus showing perfectly matched execution- and observation-related activity, could be the most appropriate elements to underpin the lowest-level forward/inverse models. In addition, given that superior layers develop from these basic models, the discharge properties of these neurons might play a critical role in the generation of the mirror visual response. This gives support to the theory which asserts that the observation of the agent's own acting effector is a fundamental step in the biological process leading to neuronal activation associated to the observation of actions performed by others (Rizzolatti and Fadiga, 1998).

The hypothesis hereby proposed is that, through the forward models normally guiding action execution, the motor system progressively extracts motor-invariant (goal-related) visual signals from the repetitive experience of performing one given action from slightly different perspectives or under conditions implying variability in the availability of the visual information relevant to the action. These visual signals that continuously change, for instance, depending on the relative

position of the head and the eye with respect to the acting hand or the target object, would be generalized by virtue of the fact that they are generated by very similar motor programs, all issued to achieved the same goal. Once this generalization process, that is supposed to play a relevant part not only during development but also during learning of new motor acts in adults, is sufficiently established, it would be then gradually transferred also to actions performed by others. In so doing, the visual representation of a given observed action would gain access to the corresponding motor representation due to the coherent action description that the observer has previously acquired through the visuomotor link concerning his/her own movements. In computational terms, the more similar the observer's hyper-MOSAIC is to the actor's hyper-MOSAIC, the easier it will be to make associations between them. These associations would be at the basis of the *recognition* operations played by mirror neurons and the flash-related effects found in this study, confirming that in area F5 there exist neurons that specifically respond when the agent observes his/her own movement, would represent the mechanism through which visual signals mapped onto the own motor programs are progressively acquired.

Additional experiments are required to more deeply explore this complex topic, such as studying the response of these neurons when visual information about the ongoing movement is disrupted and extending the testing to F5 mirror neurons. It is nevertheless interesting to note that experiments performed in artificial robotic systems aiming at simulating the development of mirror neurons through the observation of one's own hand during execution of grasping (Craighero et al. 2007; Metta et al. 2006;) seem to confirm this hypothesis.

Flash-related modulations in area F1

Despite that many studies, principally conducted on humans, have reported observation-evoked responses also in primary motor cortex, there is to date no evidence about the existence of mirror neurons in this area. These F1 modulations have been proposed to be not functional but

simply a reflection of the strong cortico-cortical interconnections with area F5 (Fadiga et al. 1995, Kilner and Frith 2007). It is well known that F5 can influence hand muscles via its dense projections to F1 (Dum and Strick 2005). Conditioning F5 stimulation results in significant facilitation of F1 corticospinal activity and, consequently, of responses in hand motoneurons (Cerrri et al. 2003; Schmidlin et al. 2008; Shimazu et al. 2004). Hence, according to this interpretation, F1 modulation during action observation could be considered as an effect of the simultaneous strong activation of area F5. An alternative hypothesis is that F1 neurons might play a specific functional role, by representing the observed actions in a different coordinate system with respect to that used by F5. In particular, it might be that whereas F5 decodes the extrinsic features of the observed action (i.e., the relative positions of the hand and of the target in space), F1 describes the intrinsic pattern of muscle activation involved in the action, similarly to what is coded by the two areas during the actual action execution (Kakei et al. 2001). Specific experiments should be carried out to test both hypotheses. However, the poor action observation-related activation of F1 found in the present study, strongly suggests that it may be rather the reflective result of the more significant modulation characterizing neuronal responses in F5.

Conclusions

By this work we demonstrate that ventral premotor area F5 contains visuomotor neurons selectively strengthening their response during continuous or transient vision of the monkey's own grasping movement. These findings confirm that F5, as well as area AIP in the parietal lobe, is crucial for the visual control of handgrip formation during grasping. Furthermore, our results lay the ground for a visuomotor theory about the generation of mirror neurons. The specific observation-evoked neuronal responses described here can be thought of as the key step for transferring the meaning attributed to our own movements to actions performed by other individuals, both during development and learning of new actions.

ACKNOWLEDGMENTS

We thank Professor G. Spidalieri for valuable comments on an earlier version of the manuscript.

GRANTS

This study was supported by the Italian Ministry of Education, by E.C. grants CONTACT (NEST Project 5010), ROBOTCUB (IST-004370) and POETICON (ICT-215843) and by Fondazione Cassa di Risparmio di Ferrara.

REFERENCES

1. **Bays PM and Wolpert DM.** Computational principles of sensorimotor control that minimize uncertainty and variability. *J Physiol* 578: 387-96, 2007.
2. **Bezdek JC, Ehrlich R and Full W.** FCM: Fuzzy C-Means Algorithm. *Computers and Geoscience* 10: 191–203, 1984.
3. **Caetano G, Jousmaki V and Hari R.** Actor's and observer's primary motor cortices stabilize similarly after seen or heard motor actions. *Proc Natl Acad Sci U S A* 104: 9058-62, 2007.
4. **Carr L, Iacoboni M, Dubeau MC, Mazziotta JC and Lenzi GL.** Neural mechanisms of empathy in humans: a relay from neural systems for imitation to limbic areas. *Proc Natl Acad Sci U S A* 100: 5497-502, 2003.
5. **Cerri G, Shimazu H, Maier MA and Lemon RN.** Facilitation from ventral premotor cortex of primary motor cortex outputs to macaque hand muscles. *J Neurophysiol* 90(2): 832-842, 2003.
6. **Cheng Y, Meltzoff AN and Decety J.** Motivation modulates the activity of the human mirror-neuron system. *Cereb Cortex* 17: 1979-86, 2007.
7. **Churchill A, Hopkins B, Ronqvist L and Vogt S.** Vision of the hand and environmental context in human prehension. *Exp Brain Res* 134: 81-9, 2000.
8. **Craighero L, Metta G, Sandini G and Fadiga L.** The mirror-neurons system: data and models. *Prog Brain Res* 164: 39-59, 2007.
9. **di Pellegrino G, Fadiga L, Fogassi L, Gallese V and Rizzolatti G.** Understanding motor

- events: a neurophysiological study. *Exp Brain Res* 91: 176-80, 1992.
10. **Dum RP and Strick PL.** Frontal lobe inputs to the digit representations of the motor areas on the lateral surface of the hemisphere. *J Neurosci* 25: 1375-86, 2005.
 11. **Fadiga L, Fogassi L, Pavesi G and Rizzolatti G.** Motor facilitation during action observation: a magnetic stimulation study. *J Neurophysiol* 73: 2608-11, 1995.
 12. **Fogassi L, Ferrari PF, Gesierich B, Rozzi S, Chersi F and Rizzolatti G.** Parietal lobe: from action organization to intention understanding. *Science* 308: 662-7, 2005.
 13. **Fogassi L, Gallese V, Buccino G, Craighero L, Fadiga L and Rizzolatti G.** Cortical mechanism for the visual guidance of hand grasping movements in the monkey: A reversible inactivation study. *Brain* 124: 571-86, 2001.
 14. **Fogassi L and Luppino G.** Motor functions of the parietal lobe. *Curr Opin Neurobiol* 15: 626-31, 2005.
 15. **Gallese V, Fadiga L, Fogassi L and Rizzolatti G.** Action recognition in the premotor cortex. *Brain* 119 (Pt 2): 593-609, 1996.
 16. **Gawne TJ, Kjaer TW and Richmond BJ.** Latency: another potential code for feature binding in striate cortex. *J Neurophysiol* 76: 1356-60, 1996.
 17. **Gentilucci M, Toni I, Chieffi S and Pavesi G.** The role of proprioception in the control of prehension movements: a kinematic study in a peripherally deafferented patient and in normal subjects. *Exp Brain Res* 99: 483-500, 1994.
 18. **Iacoboni M, Molnar-Szakacs I, Gallese V, Buccino G, Mazziotta JC and Rizzolatti G.** Grasping the intentions of others with one's own mirror neuron system. *PLoS Biol* 3: e79,

2005.

19. **Jackson SR, Jackson GM and Rosicky J.** Are non-relevant objects represented in working memory? The effect of non-target objects on reach and grasp kinematics. *Exp Brain Res* 102: 519-30, 1995.
20. **Jakobson LS and Goodale MA.** Factors affecting higher-order movement planning: a kinematic analysis of human prehension. *Exp Brain Res* 86: 199-208, 1991.
21. **Jeannerod M.** The formation of finger grip during prehension. A cortically mediated visuomotor pattern. *Behav Brain Res* 19: 99-116, 1986.
22. **Jeannerod M, Arbib MA, Rizzolatti G and Sakata H.** Grasping objects: the cortical mechanisms of visuomotor transformation. *Trends Neurosci* 18: 314-20, 1995.
23. **Kakei S, Hoffman DS and Strick PL.** Direction of action is represented in the ventral premotor cortex. *Nat Neurosci* 4: 1020-5, 2001.
24. **Kilner JM and Frith CD.** A possible role for primary motor cortex during action observation. *Proc Natl Acad Sci U S A* 104: 8683-4, 2007.
25. **Lewicki MS.** A review of methods for spike sorting: the detection and classification of neural action potentials. *Network* 9: R53-78, 1998.
26. **Liu Y and Rouiller EM.** Mechanisms of recovery of dexterity following unilateral lesion of the sensorimotor cortex in adult monkeys. *Exp Brain Res* 128: 149-59, 1999.
27. **Luppino G, Murata A, Govoni P and Matelli M.** Largely segregated parietofrontal connections linking rostral intraparietal cortex (areas AIP and VIP) and the ventral premotor cortex (areas F5 and F4). *Exp Brain Res* 128: 181-187, 1999.

28. **Matelli M, Camarda R, Glickstein M and Rizzolatti G.** Afferent and efferent projections of the inferior area 6 in the macaque monkey. *J Comp Neurol* 251: 281-98, 1986.
29. **Metz CE.** Basic principles of ROC analysis. *Semin Nucl Med* 8: 283-98, 1978.
30. **Metta G, Sandini G, Natale L, Craighero L and Fadiga L.** Understanding mirror neurons: a bio-robotic approach. *Interaction Studies* 7(2): 197-232, 2006.
31. **Miall RC.** Connecting mirror neurons and forward models. *Neuroreport* 14: 2135-7, 2003.
32. **Murata A, Fadiga L, Fogassi L, Gallese V, Raos V and Rizzolatti G.** Object representation in the ventral premotor cortex (area F5) of the monkey. *J Neurophysiol* 78: 2226-30, 1997.
33. **Murata A, Gallese V, Kaseda M and Sakata H.** Parietal neurons related to memory-guided hand manipulation. *J Neurophysiol* 75: 2180-6, 1996.
34. **Murata A, Gallese V, Luppino G, Kaseda M and Sakata H.** Selectivity for the shape, size, and orientation of objects for grasping in neurons of monkey parietal area AIP. *J Neurophysiol* 83: 2580-601, 2000.
35. **Muthukumaraswamy SD and Johnson BW.** Primary motor cortex activation during action observation revealed by wavelet analysis of the EEG. *Clin Neurophysiol* 115: 1760-6, 2004.
36. **Nelissen K, Luppino G, Vanduffel W, Rizzolatti G and Orban GA.** Observing others: multiple action representation in the frontal lobe. *Science* 310: 332-6, 2005.
37. **Perrett DI, Harries MH, Bevan R, Thomas S, Benson PJ, Mistlin AJ, Chitty AJ, Hietanen JK and Ortega JE.** Frameworks of analysis for the neural representation of animate objects and actions. *J Exp Biol* 146: 87-113, 1989.
38. **Petrides M and Pandya DN.** Projections to the frontal cortex from the posterior parietal

- region in the rhesus monkey. *J Comp Neurol* 228: 105-16, 1984.
39. **Rand MK, Lemay M, Squire LM, Shimansky YP and Stelmach GE.** Role of vision in aperture closure control during reach-to-grasp movements. *Exp Brain Res* 181: 447-60, 2007.
 40. **Raos V, Umilta MA, Gallese V and Fogassi L.** Functional properties of grasping-related neurons in the dorsal premotor area F2 of the macaque monkey. *J Neurophysiol* 92: 1990-2002, 2004.
 41. **Raos V, Umilta MA, Murata A, Fogassi L and Gallese V.** Functional properties of grasping-related neurons in the ventral premotor area F5 of the macaque monkey. *J Neurophysiol* 95: 709-29, 2006.
 42. **Rizzolatti G, Camarda R, Fogassi L, Gentilucci M, Luppino G and Matelli M.** Functional organization of inferior area 6 in the macaque monkey. II. Area F5 and the control of distal movements. *Exp Brain Res* 71: 491-507, 1988.
 43. **Rizzolatti G and Fadiga L.** Grasping objects and grasping action meanings: the dual role of monkey rostroventral premotor cortex (area F5). *Novartis Found Symp* 218: 81-95; discussion 95-103, 1998.
 44. **Rizzolatti G, Fadiga L, Gallese V and Fogassi L.** Premotor cortex and the recognition of motor actions. *Brain Res Cogn Brain Res* 3: 131-41, 1996.
 45. **Rizzolatti G, Gentilucci M, Camarda RM, Gallese V, Luppino G, Matelli M and Fogassi L.** Neurons related to reaching-grasping arm movements in the rostral part of area 6 (area 6a beta). *Exp Brain Res* 82: 337-50, 1990.
 46. **Rizzolatti G and Luppino G.** The cortical motor system. *Neuron* 31: 889-901, 2001.

47. **Sakata H, Taira M, Murata A and Mine S.** Neural mechanisms of visual guidance of hand action in the parietal cortex of the monkey. *Cereb Cortex* 5: 429-38, 1995.
48. **Schettino LF, Adamovich SV and Poizner H.** Effects of object shape and visual feedback on hand configuration during grasping. *Exp Brain Res* 151: 158-66, 2003.
49. **Schmidlin E, Brochier T, Maier MA, Kirkwood PA and Lemon RN.** Pronounced reduction of digit motor responses evoked from macaque ventral premotor cortex after reversible inactivation of the primary motor cortex hand area. *J Neurosci* 28(22): 5772-83, 2008.
50. **Schmitzer-Torbert N, Jackson J, Henze D, Harris K and Redish AD.** Quantitative measures of cluster quality for use in extracellular recordings. *Neuroscience* 131: 1-11, 2005.
51. **Shimazu H, Maier MA, Cerri G, Kirkwood PA and Lemon RN.** Macaque ventral premotor cortex exerts powerful facilitation of motor cortex outputs to upper limb motoneurons. *J Neurosci* 24: 1200-11, 2004.
52. **Szabo J and Cowan WM.** A stereotaxic atlas of the brain of the cynomolgus monkey (*Macaca fascicularis*). *J Comp Neurol* 222: 265-300, 1984.
53. **Tkach D, Reimer J and Hatsopoulos NG.** Congruent activity during action and action observation in motor cortex. *J Neurosci* 27: 13241-50, 2007.
54. **Umiltà MA, Brochier T, Spinks RL and Lemon RN.** Simultaneous recording of macaque premotor and primary motor cortex neuronal populations reveals different functional contributions to visuomotor grasp. *J Neurophysiol* 98: 488-501, 2007.
55. **Umiltà MA, Kohler E, Gallese V, Fogassi L, Fadiga L, Keysers C and Rizzolatti G.** I

- know what you are doing. a neurophysiological study. *Neuron* 31: 155-65, 2001.
56. **Wallis JD and Miller EK (2003)**. From rule to response: neuronal processes in the premotor and the prefrontal cortex. *J Neurophysiol* 83: 2639-2648, 2003.
 57. **Winges SA, Weber DJ and Santello M**. The role of vision on hand preshaping during reach to grasp. *Exp Brain Res* 152: 489-98, 2003.
 58. **Wolpert DM, Doya K and Kawato M**. A unifying computational framework for motor control and social interaction. *Philos Trans R Soc Lond B Biol Sci* 358: 593-602, 2003.
 59. **Wolpert DM and Ghahramani Z**. Computational principles of movement neuroscience. *Nat Neurosci* 3 Suppl: 1212-7, 2000.

FIGURE LEGENDS

Figure 1. Experimental setup. A: Lateral view of the behavioral apparatus, requiring the monkey to perform a reach-to-grasp task. B: Demonstration of the precision grip that the monkey had to execute in order to open the door of the food container. C: The target door was covered by an outer sliding door that the experimenter opened at each trial onset, giving the monkey a go-signal to start moving the hand from the resting position. D: Schematic representation of the time sequence of task events under the 4 experimental conditions. Line deflections indicate light or flash “on” with respect to darkness. In the *PT flash* condition, flash delivery is located at the median time across trials for both animals. Grey region around PT flash represents variability (Inter-Quartile Range) of time of flash presentation, depending on the instant at which the hand crossed the infrared barrier located 10 cm in front of the food container.

Figure 2. A: Average kinematic parameters (maximal velocity, maximal grip aperture, deceleration time, aperture-closure time) recorded for each condition (*Light 2* condition is also included) during the behavioral experiment conducted with MK1. Deceleration and aperture closure times are respectively measured as the intervals from the time of maximal velocity and from the time of maximal grip aperture to handle touch instant. B: Wrist velocity (dashed lines) and grip aperture (solid lines) recorded over time for each condition. Asterisks represent significant differences (*Kruskal-Wallis test*, 5% alpha level) of *D*, *PT flash* or *T flash* condition with respect to either or both light conditions, as specifically indicated for each plot.

Figure 3. Maps of penetration sites. A, B: Surface location of the electrode penetrations in both hemispheres of MK1. C: Penetrations in the left hemisphere of MK2. D: Lateral view of the brain surface reconstruction of MK2 (encircled region shows the position of the recording chamber). Filled symbols in the maps indicate sites where intracortical microstimulation (ICMS) elicited hand movements at different current intensity thresholds. The size of the circles is correlated with the value of the lowest threshold found in each penetration, as indicated in the key of the figure. Unfilled symbols indicate sites not tested with ICMS. Each color refers to the specific body part controlled by the neurons encountered in each penetration. AS, arcuate sulcus; CS, central sulcus. Inset plots indicate penetrations (grey dots) where neurons were recorded while the monkeys were performing the reach-to-grasp task.

Figure 4. Single units exemplifying the most significant F5 and F1 neuronal categories determined by the running *t-test* analysis comparing *L* (grey) vs. *D* (black) firing rates. The first 1500 ms of activity, aligned to time of handle touch (solid vertical line), are shown. Spike density plots are obtained by first smoothing each trial firing rate (spikes/sec, 5-ms bin width) by a Gaussian kernel function (20-ms window width) and then averaging across trials within each condition. Traces represent mean single-neuron response \pm 1 S.E.M. in the *L* and *D* conditions. Symbols on top of traces indicate trial bins where *t-test* result was significant (5% alpha level). Top raster plots represent the respective spike trains recorded from the neuron in the 12 trials of the two conditions. A: Neurons showing a $L > D$ modulation in the *pre-touch* sub-epoch (shaded area). B: *L*-modulated neurons around the instant at which the hand touched the handle. C: Neurons expressing *L*-selectivity in both *pre-* and *post-touch* sub-epochs (shaded area). D: Stem plots exemplifying the running *t-test* analysis performed on the *L-* and *D-*related activity of the neurons shown in (C). The activity of the neurons in the two conditions is represented by the index $(D-L)/(D+L)$; lines extending from the baseline (index = 0) upward and downward respectively represent $D > L$ and $L > D$ modulations computed at each 100-ms bin. Red and black lines indicate significant ($P < 0.05$) and non-significant modulations, respectively. A given neuron was considered as *L-* or *D-*selective if it displayed the same significant modulation in at least three consecutive bins. The same analysis was employed to detect *PT flash/T flash*-selective neurons.

Figure 5. Single units exemplifying other significant F5 and F1 neuronal categories determined by the running *t-test* analysis comparing *L* (grey) vs. *D* (black) firing rates. A: Neurons showing a $D > L$ modulation in the *post-touch* sub-epoch (shaded area). B: Neurons with higher firing rates in the *D* condition throughout *epoch 2* (shaded area). C: Neurons with a “*spurious*” effect, exhibiting opposite modulations within *epoch 2*, as a result of a shift in activity between *L* and *D* conditions (for descriptive purposes, the activity recorded during the whole trial period is presented). Conventions as in Fig. 4.

Figure 6. A: Average activity of *pre-touch* light-responsive neurons in area F5 and F1. The first 1500 ms of activity aligned to time of handle touch (solid vertical line) are shown. Population spike density plots are obtained by first normalizing the single-neuron smoothed data (Gaussian kernel function with window width set at 30 ms) to the absolute maximum level of activity observed across all 4 conditions and then averaging the result across all units in the populations. Traces represent the *L-* (grey) and *D-* (black) related average response \pm 1 S.E.M of the population. Symbols on top of traces indicate trial bins where the running *t-test* result was significant (5% alpha level). B: Time course of ROC values for the F5 and F1 *pre-touch* light-selective populations shown in (A). Traces are obtained

averaging across neurons the area under the ROC curve, comparing *L* and *D* firing rates in a sliding 100-ms bin stepped by 20 ms. C: Histograms showing the distribution of F5 and F1 single-neuron ROC area values in the *pre-touch* sub-epoch (corresponding shaded area in the plot shown in (B)). ROC areas higher than 0.5 (grey) indicate neurons conveying more light- than dark-related information; ROC values lower than 0.5 (black) represent neurons expressing information in the opposite direction. Note that the presence of black bars is due to the not very restrictive criterion used for selecting light-responsive neurons, requiring selectivity in at least 3 consecutive bins within the *pre-touch* sub-epoch. D: Mean latency and peak times for the *L*- and *D*-related responses of F5 and F1 *pre-touch L*-selective populations. Note that latency is computed as the time to half the peak of discharge, meaning that it is more related to the rise time of activity to the peak, rather than to the actual onset of the neuronal response. Asterisks on top indicate statistically significant differences (*Student's t*-test, 5% alpha level). E: Line fitting of the *L*- and *D*-related response of F5 and F1 *pre-touch L*-selective neurons in a 300-ms window prior to touch, both at the population (left) and at the single-unit level (right). The regression analysis returned similar slope-intercept *L* and *D* functions for the F1 population, while F5 population displayed very different ramping activities. F: Histograms representing the distribution of differences in the slope of the *L* and *D* response profiles for neurons in area F5 and F1.

Figure 7. Examples of F5 and F1 flash-responsive single neurons, as assessed by the running *t*-test analysis. A: Neurons showing significantly higher firing rates during *epoch 2* of the *PT flash* condition (red) than during *epoch 2* of the *T flash* condition (blue). B: neurons specifically responding to *T flash*. Red and blue vertical lines represent the time of *PT flash* (-180 ms, -216 ms and -117 ms, respectively) and *T flash* (always at 0 ms) delivery. Mean activity during *D* (black) and *L* (grey) conditions for each neuron is shown as well. Other conventions as in Fig. 4.

Figure 8. Average activity of flash-responsive neurons in area F5 and F1. Activity in *PT flash* (red) is plotted vs. activity in *T flash* (blue) condition. A: *PT flash*-selective populations. Vertical red solid line and red shaded area around it respectively represent the median time of *PT flash* occurrence and Inter-Quartile Range (IQR) for each population (F5: -201 ms, IQR = 115 ms; F1: -133 ms, IQR = 113 ms). B: *T flash*-selective populations. Vertical blue solid lines represent the time of *T flash* occurrence (always at 0 ms). Other conventions as in Fig. 6A. C: Time course of ROC values for *PT flash*- and *T flash*-selective groups in area F5 (left) and F1 (right). Both traces are represented with positive ROC values to better contrast them. Conventions as in Fig. 6B. D: Same ROC traces as in (C) but grouped according to the type of flash selectivity (left plot: *PT flash*-responsive neurons; right plot: *T flash*-responsive neurons), to emphasize differences between areas. E: Histograms showing the distribution of single-neuron ROC area values in

both *pre-touch* (dark blue and red) and *post-touch* (pale blue and red) sub-epochs within *PT flash*- and *T flash*-responsive groups recorded from the two brain regions. ROC areas higher than 0.5 (blue) indicate neurons conveying more *T flash*- than *PT flash*-related information; ROC values lower than 0.5 (red) represent neurons expressing the opposite effect. Note that the presence of bars of the opposite color within each plot is due to the not very restricted criterion used for selecting flash-responsive neurons.

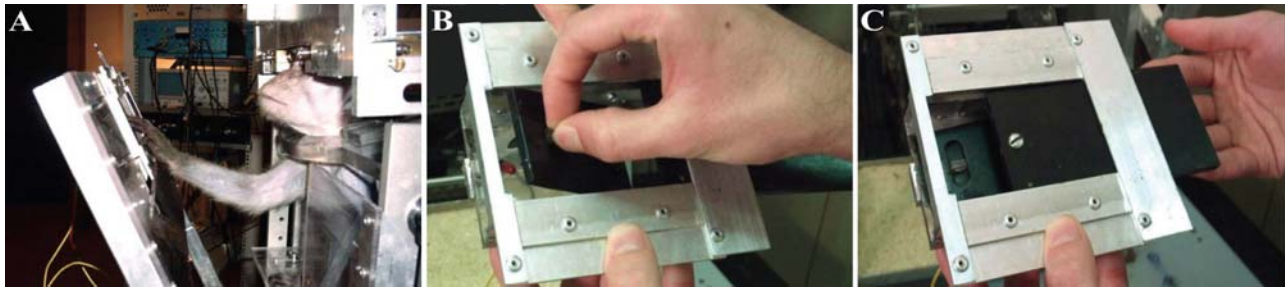
Figure 9. Average activity of flash-responsive neurons in area F5 and in area F1 across the four conditions. Activity is aligned to time of handle touch (solid line). Population spike density plots are obtained by first normalizing the single-neuron smoothed data (Gaussian kernel function with window width set to 100 ms, to better emphasize the neuronal response profile) to the absolute maximum level of activity observed across all conditions and then averaging the result across all units in the populations. Average activity in *PT flash* (red), *T flash* (blue), *L* (grey) and *D* (black) conditions is plotted for each group. A: *PT flash*-selective populations. Box plots on top of traces indicate the temporal distribution of the discharge peaks of the neurons within a population. The distance between left and right limits of the box define Inter-Quartile Range (IQR) of the sample. The line in the middle is the sample median, whiskers represent the extent of the rest of the data and red crosses are outliers. Inset plots show the temporal spread of the discharge peaks of each flash-selective group in the four conditions. IQR details are given in Tab. 3. Grey-shaded area within each plot include *pre-touch* and *post-touch* sub-epochs where statistical analyses have been performed..

Figure 10. Average activity of F5 and F1 *PT flash* and *T flash*-responsive neurons in the four experimental conditions, both during *pre-touch* and *post-touch* sub-epochs (A, B) and at the time of maximum (*Peak*) and half-maximum (*Latency*) discharge (C, D). Asterisks on top of bar plots indicate main significant differences among conditions ($P < 0.05$, LSD post-hoc tests).

TABLE 2 LEGEND

Table 2. Percentages of modulated neurons resulting from the running paired *t-test* analysis, comparing single-neuron activity in *D* vs. *L* conditions and *PT flash* vs. *T flash* conditions in a 100-ms time window shifted through the trial by 20 ms steps. Neurons are divided according to the monkey from which they were recorded (MK1 or MK2) and the specific selectivity they showed in the different time epochs. Intersection of each flash-selective neuronal group with *L*-selective neurons in the different time epochs is also shown. The percentage values always refer to the entire samples of F5 and F1 recorded neurons.

Figure 1



D

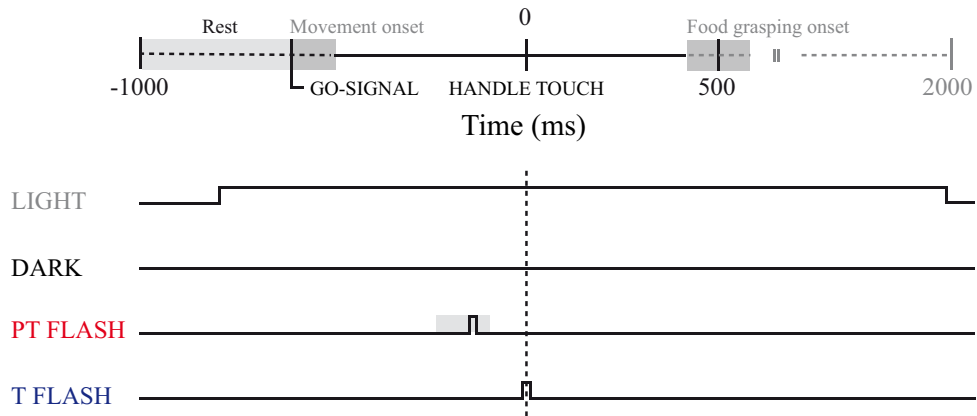


Figure 2

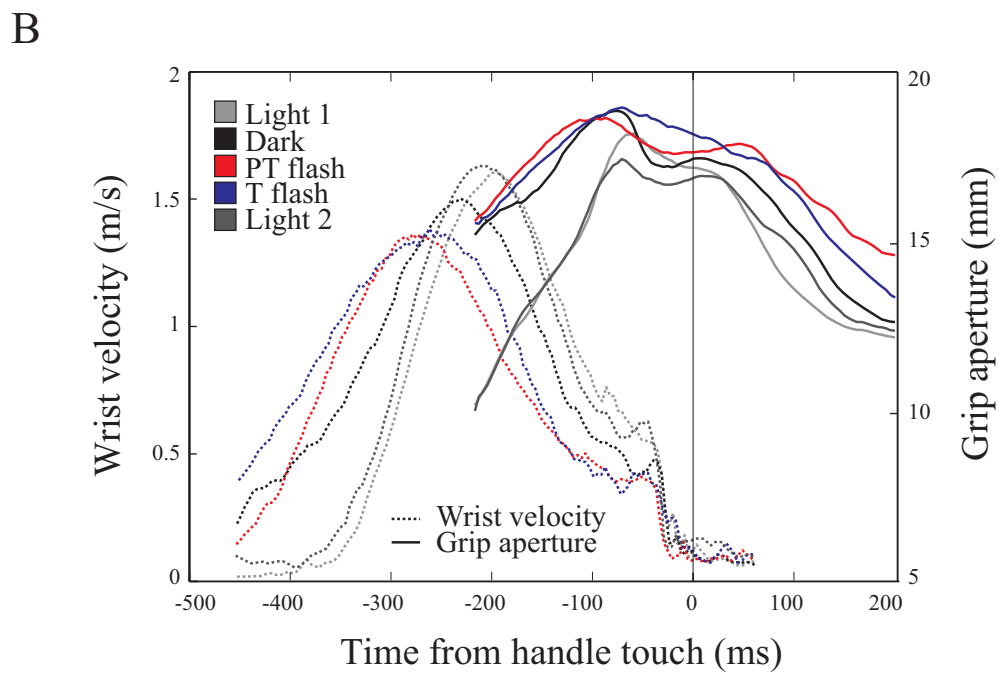
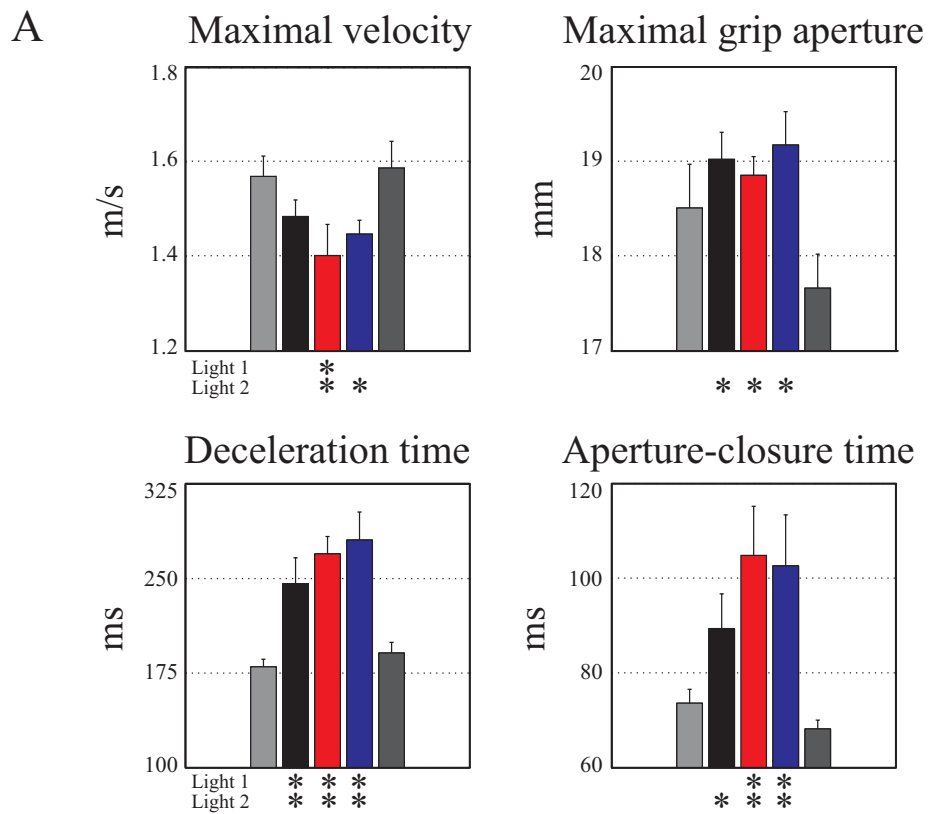


Figure 3

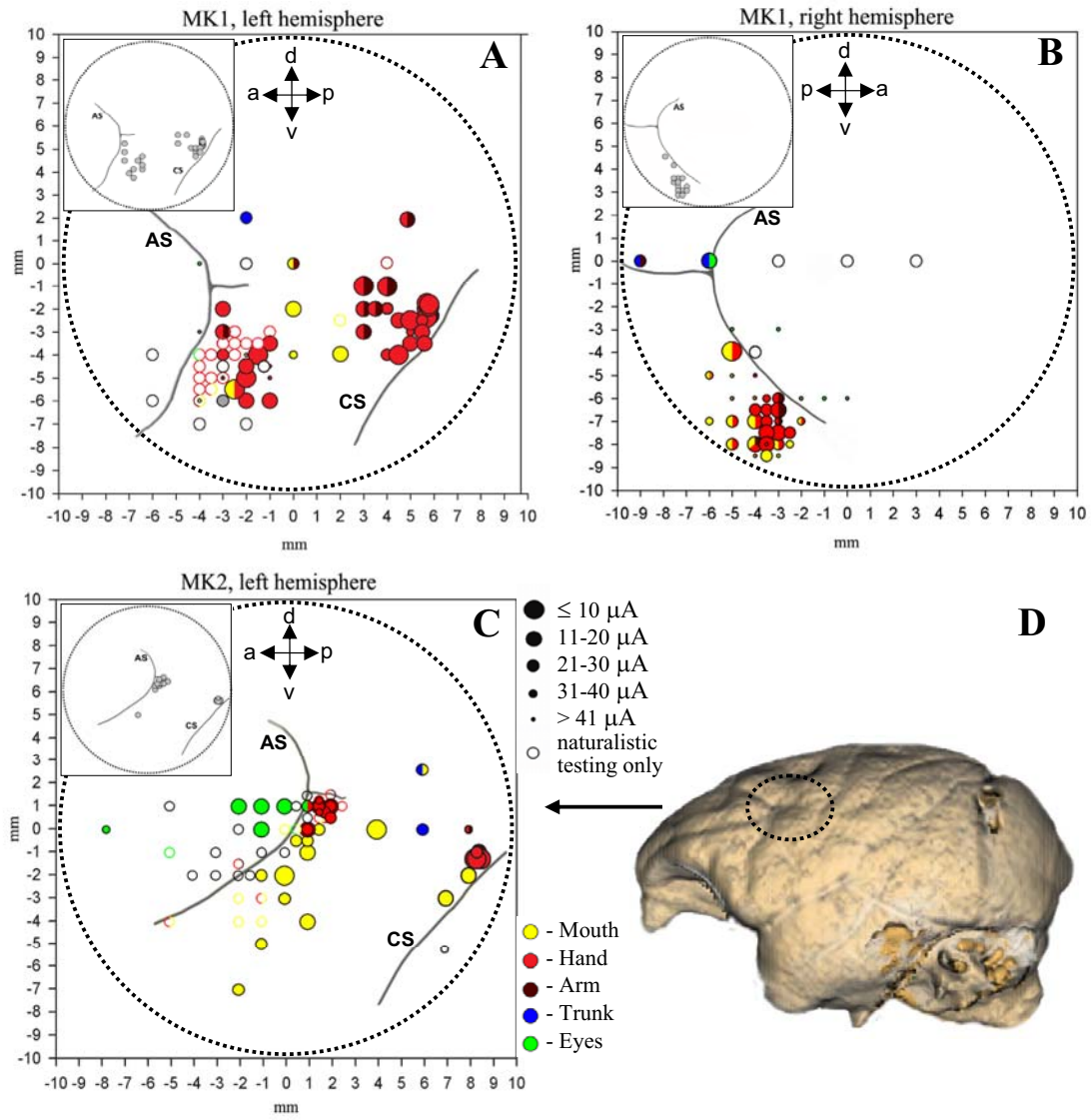


Figure 4

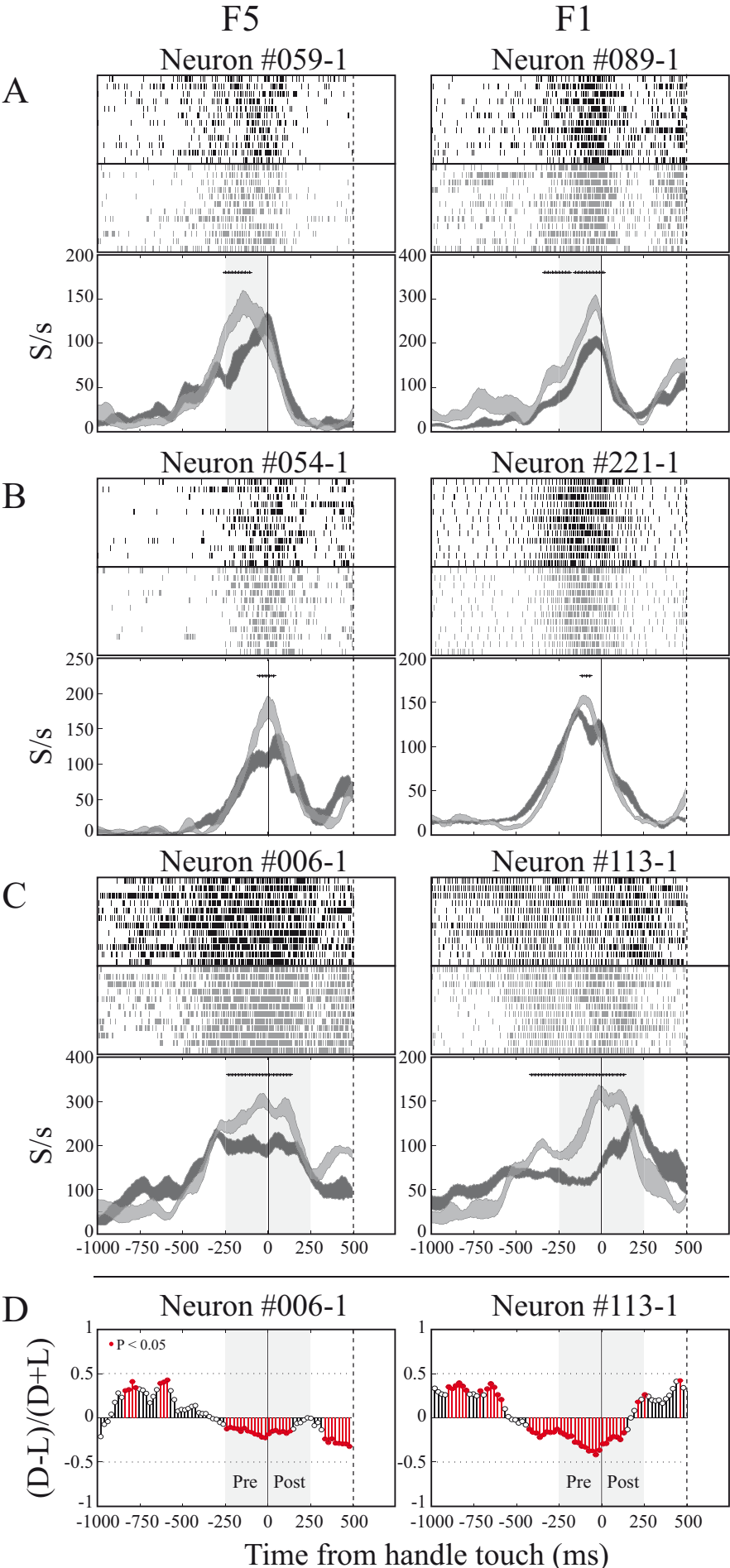


Figure 5

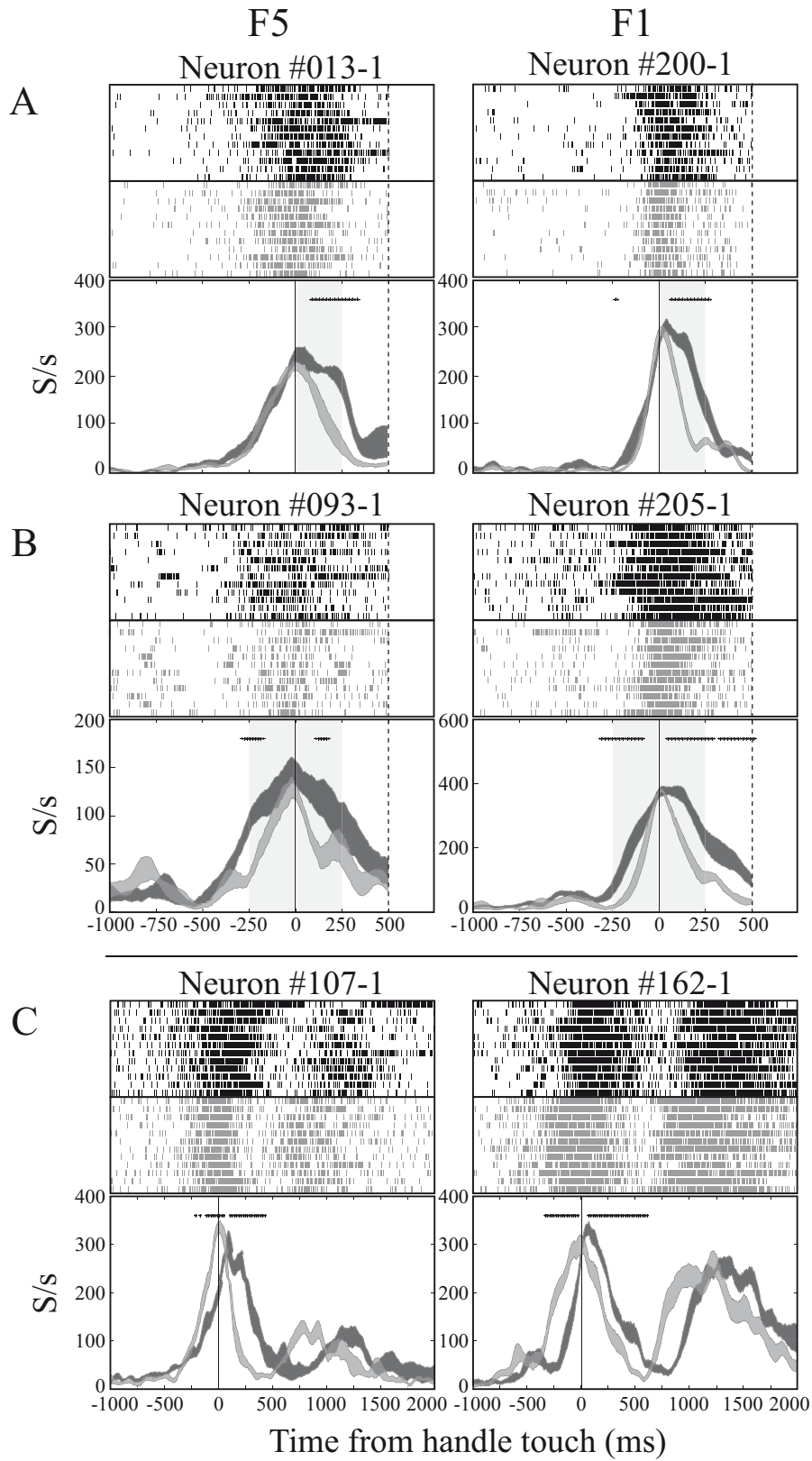


Figure 6

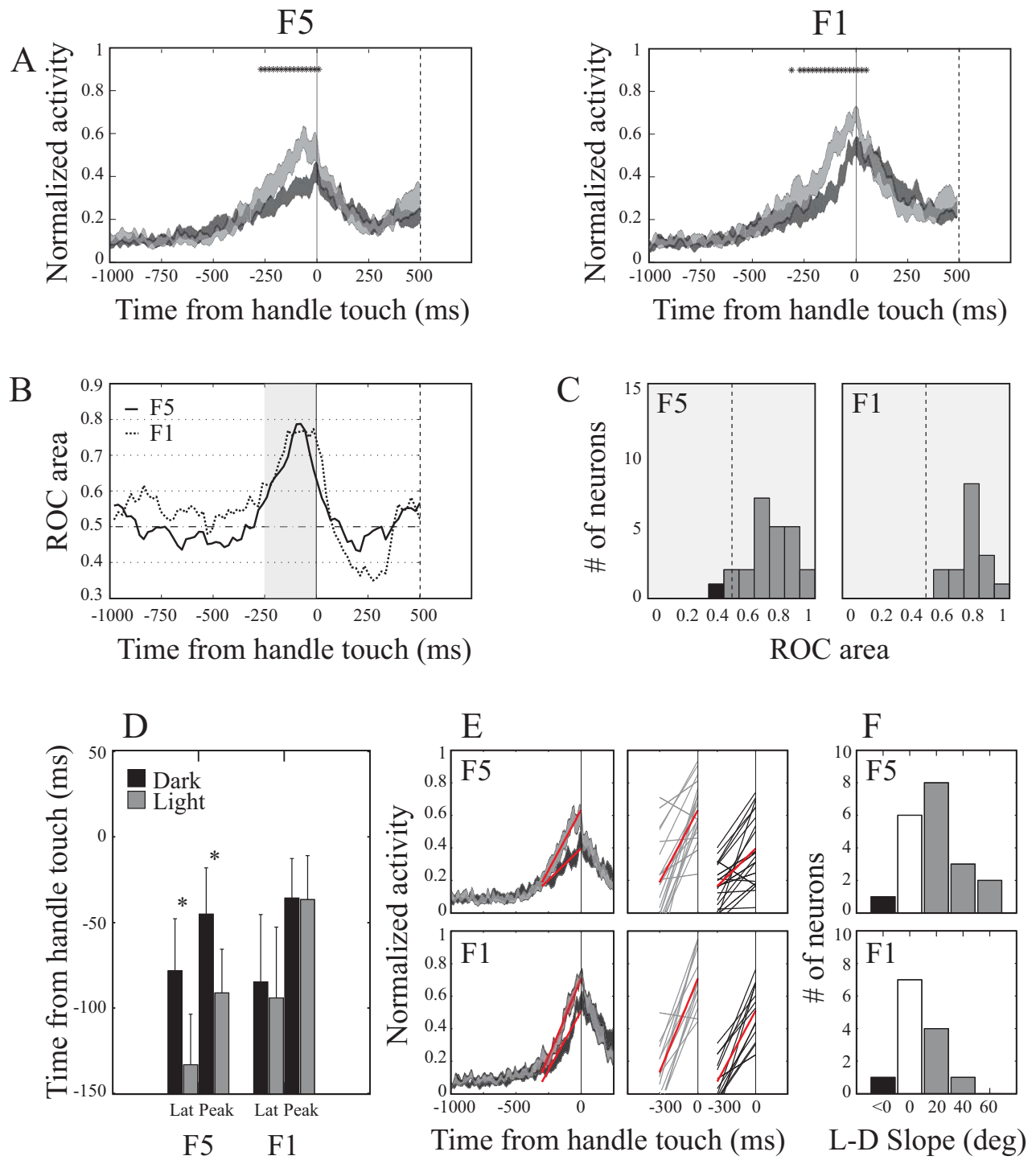


Figure 7

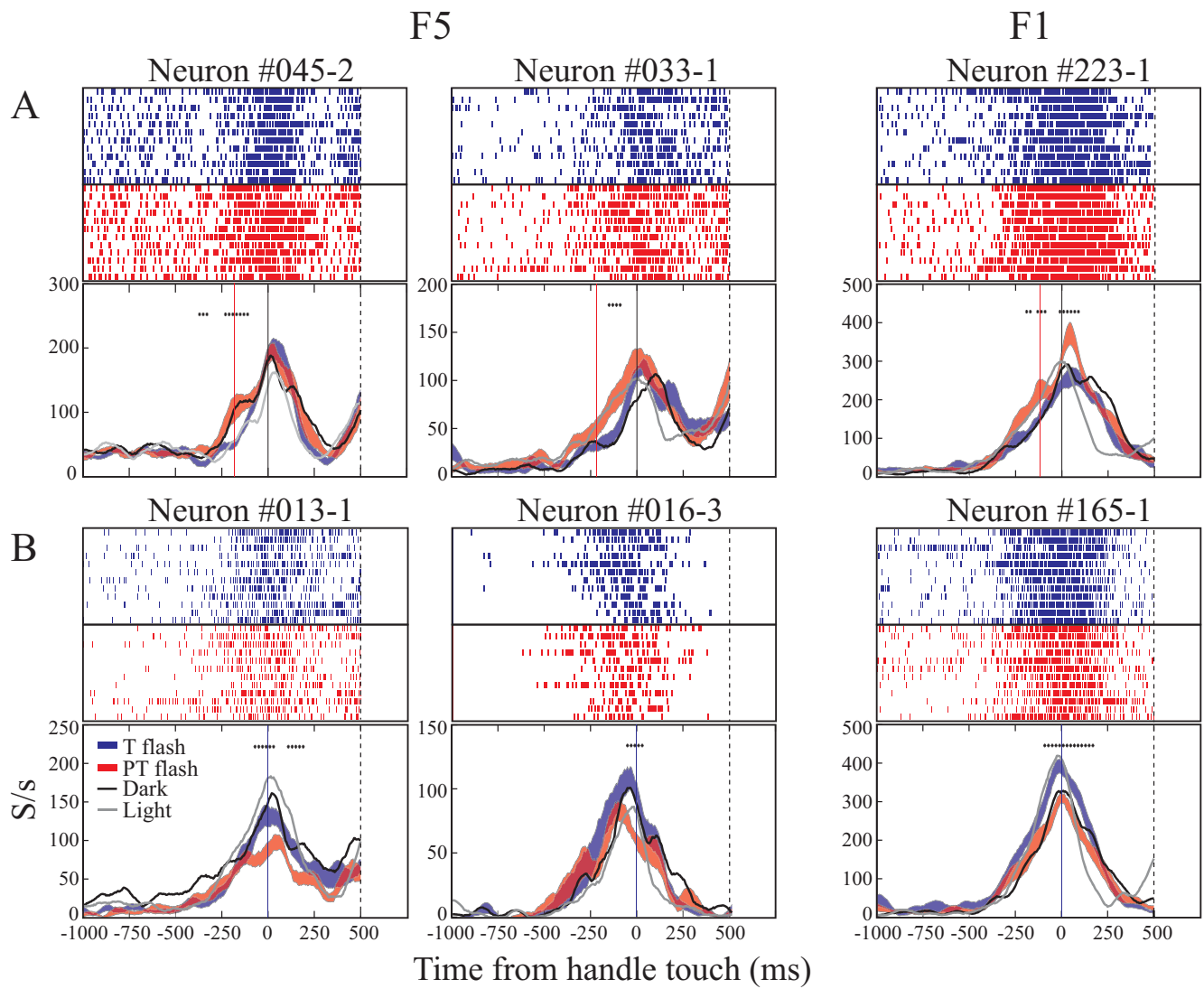


Figure 8

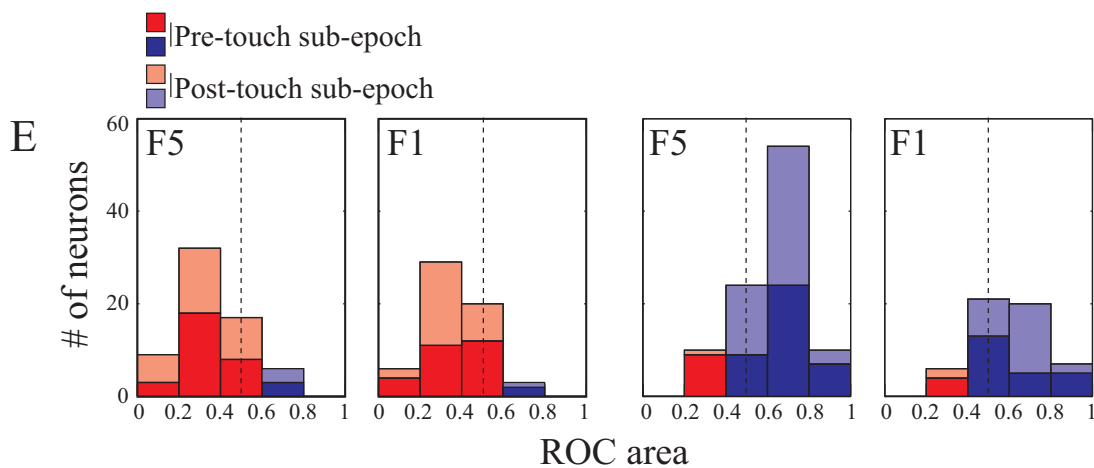
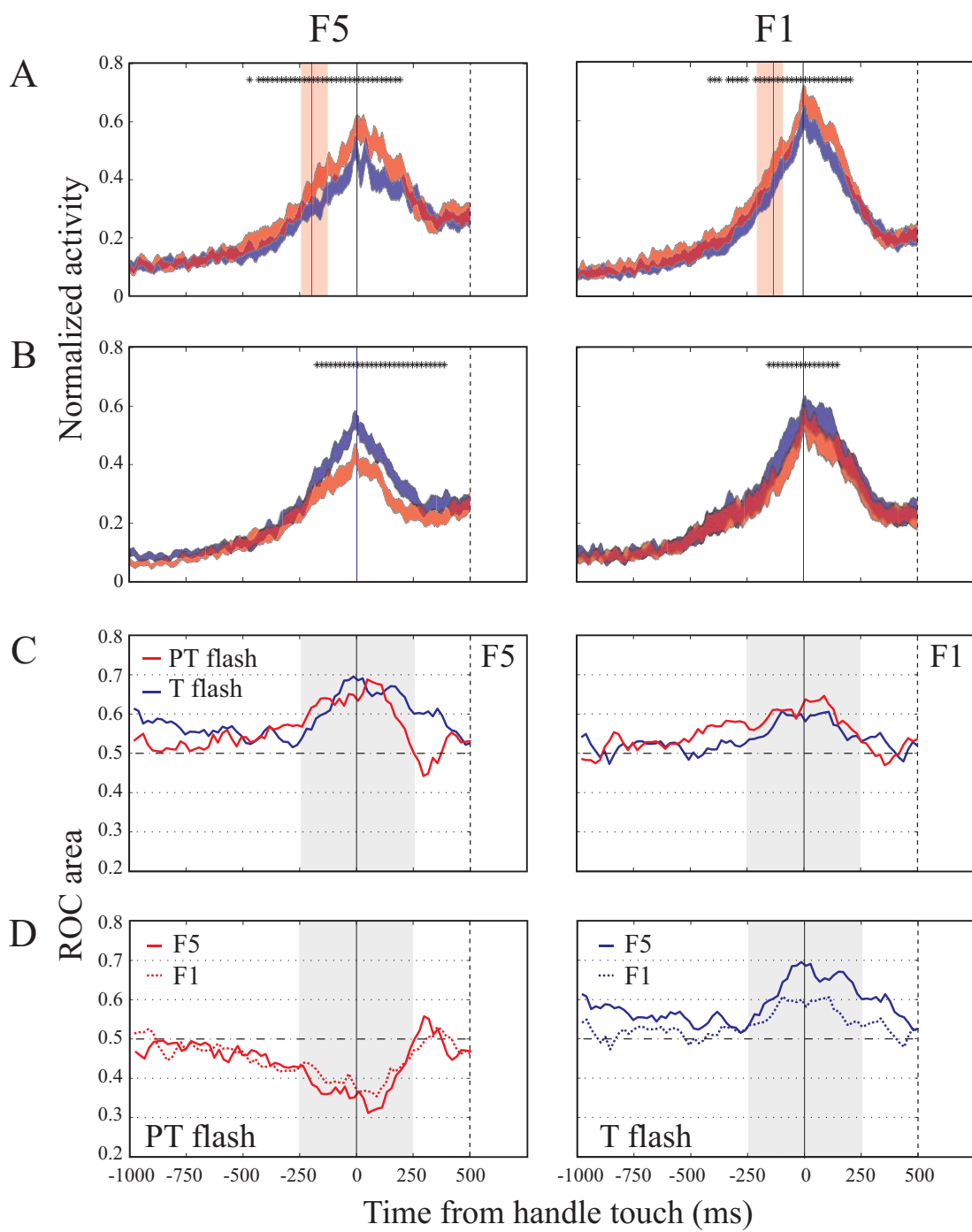


Figure 9

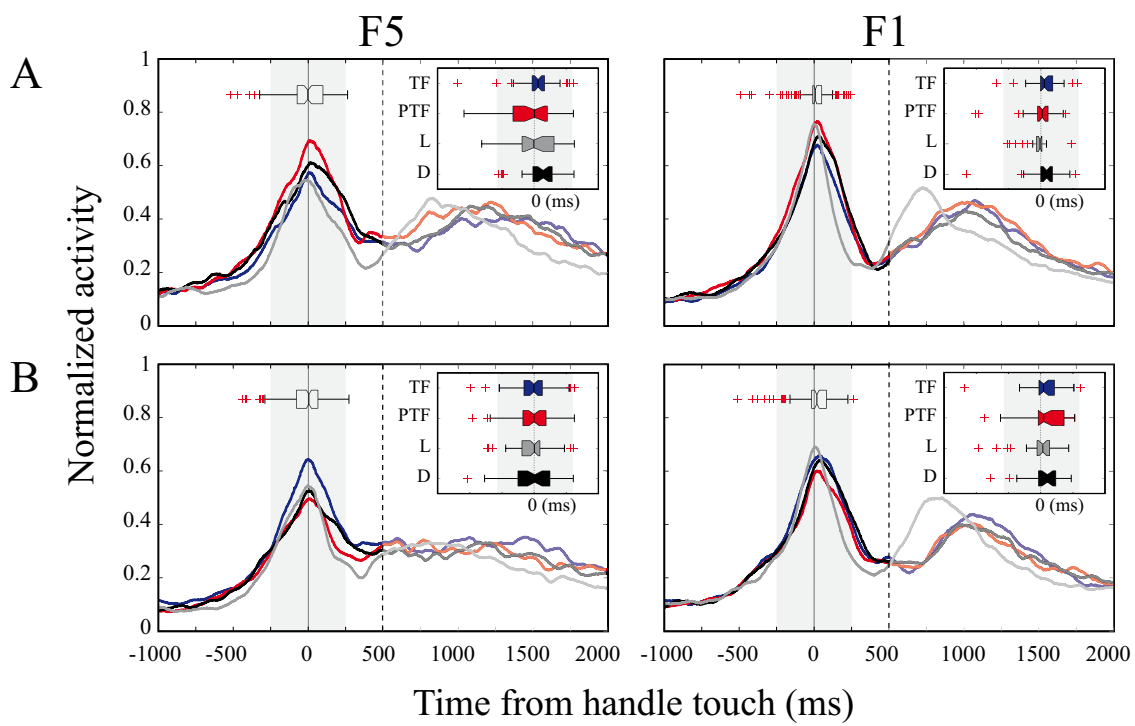


Figure 10

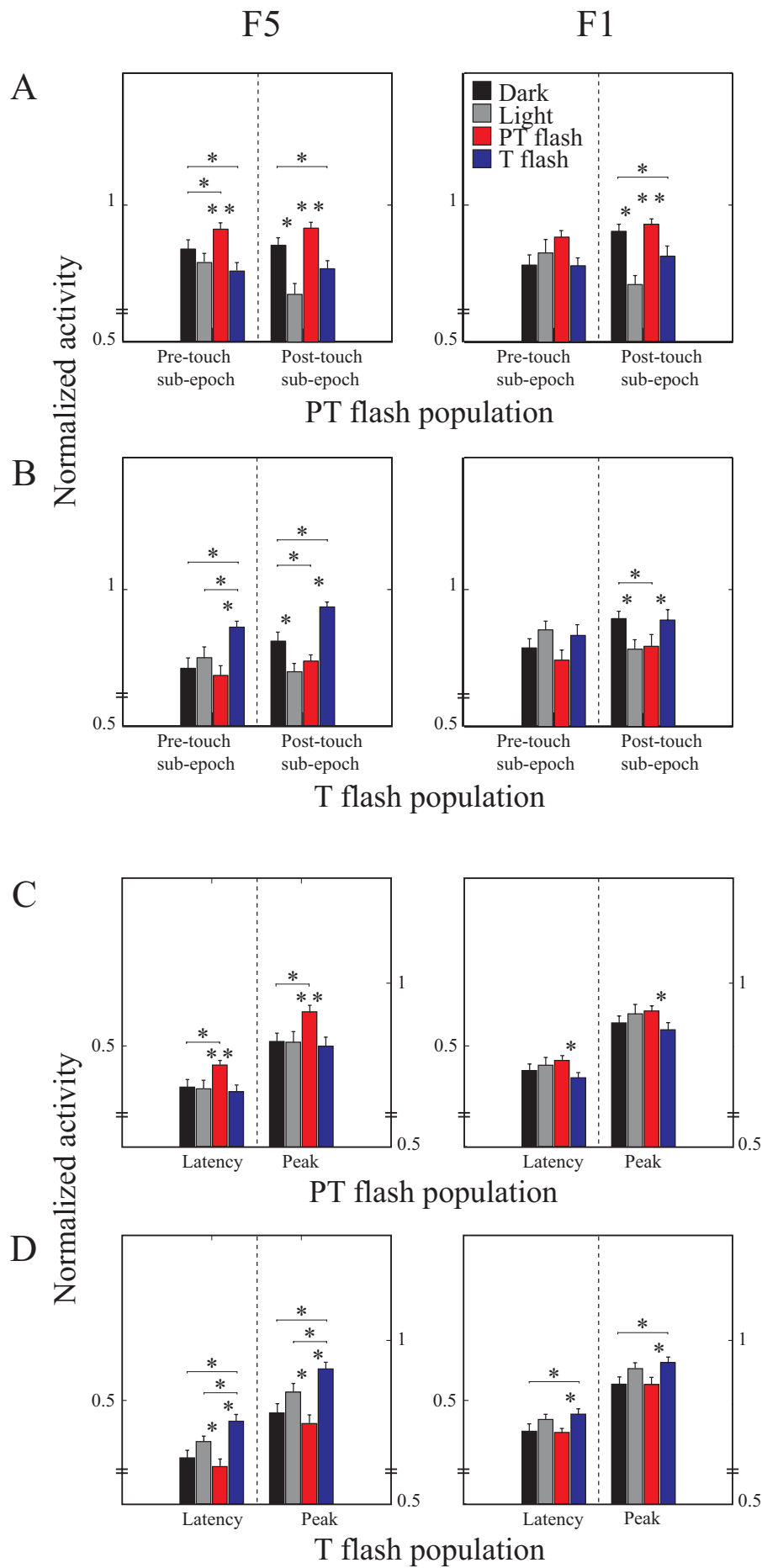


Table 1. Summary of the database.

	<i>Monkey 1</i>				<i>Monkey 2</i>			
	F5		F1		F5		F1	
	LH Right hand	RH Left hand	LH Right hand	RH	LH Right hand	RH	LH Right hand	RH
Penetrations	41	32	21	--	45	--	10	--
Recording sessions	52	62	67	--	67	--	23	--
Isolated units	67	116	204	--	112	--	32	--
Analyzed database								
<i>S</i> : session	S = 23	S = 32	S = 67	--	S = 49	--	S = 17	--
<i>N</i> : neurons	N = 38	N = 64	N = 106	--	N = 67	--	N = 22	--
PT flash delivery	-169 ms	-200 ms	-126 ms	--	-215 ms	--	-190 ms	--
(median (IQR))*	(-225/-107)	(-242/-133)	(-178/-93)	--	(-252/-167)	--	(-251/-135)	--

* Median and inter-quartile range (IQR) of times of *PT flash* delivery, according to the instant when the hand (right or left, depending on the recorded hemisphere) crossed the IR barrier before touching the door handle (temporal values are aligned to handle touch).

Table 2. Summary of main results.

		<i>Epoch 2</i>		<i>Pre-touch</i>		<i>Touch</i>		<i>Post-touch</i>		<i>Pre- + Post-touch</i>		<i>Sub-total</i>	
		<i>-250 – 250</i>		<i>-250 – 0</i>		<i>around 0</i>		<i>0 – 250</i>		<i></i>			
		<i>ms</i>		<i>ms</i>		<i>ms</i>		<i>ms</i>					
		MK1	MK2	MK1	MK2	MK1	MK2	MK1	MK2	MK1	MK2	MK1	MK2
F5													
<i>L > D</i>				13	11	3	1	5	--	4	--	25	13
				24 (14%)		4 (2%)		5 (3%)		4 (2%)		37 (22%)	
<i>D > L</i>				4	7	1	1	23	14	10	7	35	32
				11 (7%)		2 (1%)		37 (22%)		17 (10%)		67 (39%)	
<i>Modulated</i>				35		6		42		21		104 (61%)	
<i>Spurious</i>												20	10
												30 (18%)	
<i>Non-selective</i>												22	13
												35 (21%)	
Total												169 (100%)	
<i>Intersection with L > D neurons</i>													
<i>PT flash-selective</i>	23	9	3	1									
	32 (19%)		4	--	--	--	--	--	--	--	--	4 (2%)	
<i>T flash-selective</i>	29	20	2	3			4		1				
	49 (29%)		5	--	--	--	4	--	1	--	--	10 (6%)	
<i>Modulated</i>	81 (48%)												
<i>Non-selective</i>	50	38											
	88 (52%)												
Total	169 (100%)												
F1													
<i>L > D</i>				13	3	3	--	6	--	3	--	25	3
				16 (13%)		3 (2%)		6 (5%)		3 (2%)		28 (22%)	
<i>D > L</i>				4	2	--	--	21	4	10	1	35	7
				6 (5%)		--		25 (20%)		11 (9%)		42 (32%)	
<i>Modulated</i>				22		3		31		14		70 (54%)	
<i>Spurious</i>												28	6
												34 (27%)	
<i>Non-selective</i>												18	6
												24 (19%)	
Total												128 (100%)	
<i>Intersection with L > D neurons</i>													
<i>PT flash-selective</i>	24	5	1					1		1			
	29 (22%)		1	--	--	--	1	--	1	--		3 (2%)	
<i>T flash-selective</i>	23	4	5	1			1						
	27 (21%)		6	--	--	--	1	--	--	--		7 (5%)	
<i>Modulated</i>	56 (43%)												
<i>Non-selective</i>	72 (57%)												
Total	128 (100%)												

Table 3. Temporal dispersion (Inter-Quartile Range, IQR) of the discharge peaks of F5 and F1 *PT flash*- and *T flash*-selective populations in the four experimental conditions.

	<i>Peak IQR</i> (<i>ms</i>)	
	F5	F1
Flash-selective neurons	144 *	72
PT flash-selective	161	56
<i>Dark</i>	120 §	73 °
<i>Light</i>	199	34
<i>PT flash</i>	214	65 °
<i>T flash</i>	78 §	75 °
T flash-selective	134	93
<i>Dark</i>	199 ^	108
<i>Light</i>	112	79
<i>PT flash</i>	144	160 °
<i>T flash</i>	114	96
Non-selective neurons	125	123

* Significant difference (*Ansari-Bradley test* for samples with different dispersions, 5% alpha level) between F5 and F1 flash-selective neurons.

§ Significant differences with respect to *PT flash* condition within the same neuronal population.

^ Significant differences with respect to *T flash* condition within the same neuronal population.

° Significant differences with respect to *Light* condition within the same neuronal population.